MORPHOLOGY AND PROTEIN COMPOSITION OF TWO SUBLINES OF THE 13762 RAT MAMMARY ADENOCARCINOMA

By

JULIE ROBERTS CRAIK

Bachelor of Arts

University of York

York, England

1976

Submitted to the Faculty of the Graduate College
of the Oklahoma State University
in partial fulfillment of the requirements
for the Degree of
MASTER OF SCIENCE
July, 1982

MORPHOLOGY AND PROTEIN COMPOSITION OF

TWO SUBLINES OF THE 13762 RAT

MAMMARY ADENOCARCINOMA

Thesis Approved:

Ulrich Melcher

Thesis Adviser

Ta-hsiu Liao

Roger E. Koeppe

Norman N. Durham

Dean of the Graduate College

ACKNOWLEDGMENTS

I wish to thank my Research Adviser, Dr. K. L. Carraway, for giving me the opportunity to enter the field of Biochemical Research. Thanks also go to Dr. U. Melcher for his encouragement and advice on taking over responsibility for this project. I would also like to acknowledge and thank Drs. R. E. Koeppe and T. H. Liao for their valuable time spent as members of my advisory committee.

I also wish to acknowledge the invaluable technical advice of Drs. C. A. C. Carraway, R. E. Hinkley, R. W. Rubin and Ms. Carmen Castello at the Department of Anatomy, University of Miami.

I am pleased to acknowledge the friendship and support shown by Dr. Ricki Helm, Steven Hull and Goeh Jung. Special thanks go to Susan Armour for her friendship and generous hospitality.

Thanks are also extended to Sue Heil for her typing expertise.

Financial assistance and facilities provided by the Department of Biochemistry, Oklahoma State University and the Department of Anatomy, University of Miami, are gratefully acknowledged.

Thanks also go to Peter Brown for his encouragement throughout my academic career.

In addition, I wish to thank my parents, Joan and Lloyd, for their love and guidance, and my husband, Jamie, for his love, faith and patience during the preparation of this thesis.

TABLE OF CONTENTS

LIST OF FIGURES

NOMENCLATURE

Å	-	Angstrom, 10^{-8} cm
ASGP	-	Ascites sialoglycoprotein
BSA	-	Bovine serum albumin
°C	-	Degrees centigrade
CAG	-	Cytoskeletal associated glycoprotein
cm	-	Centimeter
D	-	Dimensional
DNase	-	Deoxyribonuclease
DPBS	-	Dulbecco's phosphate buffered saline (PBS containing)
EDTA	-	Ethylenediaminetetraacetic acid
EGTA	-	Ethyleneglycol-bis-(β-amino-ethyl ether) N,N'-tetraacetic acid
F-actin	-	Filamentous actin
g	-	Gravity
G-actin	-	Globular actin
GE	-	5 mM glycine, 1 mM EDTA, pH 9.5 buffer
GEM	-	5 mM glycine, 1 mM EDTA, 5 mM β-mercaptoethanol, pH 9.5 buffer
IEF	-	Isoelectric focusing
K	-	Thousand
M	-	Molar
mA	-	Milliamps
MAT	-	Mammary ascites tumor

MF - Membrane fraction, prepared in GE buffer at 4°C

MF2 - Membrane fraction 2, prepared in GEM buffer at room temperature

$MF2_c$ - Membrane fraction 2, prepared in GEM buffer at 4°C

mg - Milligram

ml - Milliliter

mM - Millimolar

MMTV - Mouse mammary tumor virus

N - Normal

NP-40 - Nonidet P-40

PAGE - Polyacrylamide gel electrophoresis

PAS - Periodic acid Schiff reagent

PBS - Phosphate buffered saline

PMSF - Phenylmethylsulfonyl fluoride

RNA - Ribonucleic acid

rpm - Revolutions per minute

SDS - Sodium dodecyl sulfate

TEM - Transmission electron microscopy

µCi - Microcurie

µg - Microgram

µl - Microliter

µm - Micrometer, 10^{-4} cm

V - Volts

v - Volume

w - Weight

CHAPTER I

INTRODUCTION

The plasma membranes of mammalian cells participate in a wide variety of cellular activities, including motility, contact inhibition of growth, immune responses and neoplastic diseases (1-4). The composition and organization of molecules at the surface of these cells are believed to be of major importance in mediating cellular responses to changes in the external environment. However, the mechanisms by which these dynamic processes may be controlled are poorly understood.

One of the most important biological observations of the early 1970's was the lateral movement of some membrane proteins, particularly glycoproteins, within the plane of the membrane. This was made possible by covalently linking fluorescent molecules to antibodies directed against cell surface antigens. Frye and Edidin (5) employed this technique very successfully. They used double immunofluorescence to investigate the membrane events which occurred in fused heterokaryons. They found that the surface components were very mobile and underwent a rapid diffusion and intermixing upon heterokaryon formation. This mobility phenomenon was readily incorporated into the "fluid mosaic model" of membrane organization, but subsequent observations soon revealed that this interpretation was too simplistic (6). The original proposal continues to provide a general working model for gross membrane structure, while new concepts have evolved to accommodate a number of

more complex phenomena.

Multivalent antibodies, or lectins, which bind to cell surface receptors can be 'tagged' with fluorescent or electron dense markers. These probes can be used to label specific membrane proteins and trace any redistribution which is induced directly or indirectly by the ligand (7). The two most striking phenomena observed in this way are patching and capping. Patching is a short range, metabolically independent redistribution of receptors. The tagged surface material, which initially has a uniform distribution, can be seen to collect in small aggregates as patching proceeds. The capping event is a metabolically dependent, long range redistribution of receptors. In this case all the tagged material becomes localized in one specific area which is termed a cap. Both types of lateral mobility are dependent upon the concentration of the ligand. In addition, both types of redistribution can usually be inhibited by reduced temperatures, or by the presence of a fixative such as glutaraldehyde (8).

The ability of a particular ligand to promote long range redistribution of receptors depends primarily upon the cell type. If the ligand is able to bind to certain cell surface molecules the ligand-receptor complexes might assemble into a cap, although this does not necessarily follow. Furthermore, if two ligands with different specificities are applied to a cell their receptors may or may not co-cap (9). These observations imply that there is some selectivity in the process of long range receptor redistribution. However, short range redistribution of at least some membrane molecules may also be selective. This hypothesis is supported by events which occur during endocytosis. In this process specific components on the cell surface

can be internalized without a general removal of membrane proteins (10). It is therefore possible that some components may be moved into or out of the area of membrane which will eventually invaginate to form an endocytic vesicle.

Unusual cell surface topology can often be correlated with a submembrane localization of cytoskeletal material. Immunofluorescence and electron microscopy studies have revealed that cytoskeletal elements, particularly microfilaments, are localized within microvilli; within areas of cells undergoing patching or capping; and beneath areas of membrane which are undergoing endocytosis (11-13). On the basis of this type of information it has been postulated that the organization of molecules at the cell surface may be controlled by their interaction with the cytoskeleton. Further evidence to support this proposal has come from experiments in which drugs were used to disrupt the cytoskeleton. Cytochalasin B causes the break-up of microfilaments, while colchicine disrupts microtubules. Both these effects can often be correlated with a perturbation of the ligand induced receptor mobility phenomenon (14).

Some of the most direct evidence in support of the proposed receptor-cytoskeleton interaction has come from studies on erythrocyte ghosts (15, 16). Fully differentiated red blood cells have relatively immobile surface components but this characteristic is not an irreversible product of their development. If these cells are subjected to hypotonic lysis membrane ghosts are produced in which the restrictive, controlling mechanism appears to be lost. In this condition membrane proteins can be induced to move in response to certain treatments such as decreased pH or trypsinization, neither of which produce similar

effects in intact cells. The bifunctional reagent dimethylmalonimidate is not able to cross-link the cytoskeletal protein spectrin in untreated ghosts. However, if the membranes are treated with lectins under conditions which cause the lectin receptors to aggregate, the spectrin can be cross-linked into high molecular weight complexes. This suggests that the aggregation of surface receptors has a transmembrane effect which causes aggregation of cytoskeletal components. The reverse situation can be observed when ghosts are treated with anti-spectrin. The antibody causes cross-linking and aggregation of spectrin with a concomitant redistribution of the surface proteins (17).

If the structural elements contained within cells can exercise specific control over the distribution of molecules at the cell surface, a transient or permanent link of at least some of the surface molecules with the cytoskeleton may be implied. Bourguignon and Singer (18) have proposed the existence of an integral membrane protein or class of proteins named X, which may be directly or indirectly linked to the cytoskeleton. Thus, X could transfer information from one side of the bilayer to the other and may play a key role in patching and capping. This model has many far reaching implications and it is therefore disappointing to note the lack of progress which has been made in identifying these X factors.

The presence of a cytoskeleton within animal cells was only really appreciated after the introduction of glutaraldehyde as a fixative for electron microscopy preparations (19). Since this important breakthrough three major constituents of the cytoskeleton have been identified in conjunction with biochemical techniques.

Microtubules are major structural components in cilia, flagella

and the mitotic spindle apparatus (20). They are long, hollow and cylindrical, with an external diameter of approximately 250 Å. These structures are assembled from subunits which contain one α and one β tubulin molecule, both of which have a molecular weight of about 54,000 daltons. Although these two proteins are not identical they have very similar amino acid sequences and are believed to have a common ancestral origin. Together the tubulins account for about 90% of the protein in microtubules. The remaining 10% contains a number of microtubule associated proteins which are currently being intensively investigated.

Intermediate filaments are approximately 100 Å in diameter and vary in composition depending upon the tissue type (21). For example, desmin, a protein with a molecular weight of 55,000 daltons, has been identified in muscle cells. Vimentin, 52,000 daltons, has been identified in fibroblasts and the keratins, 40,000 - 65,000 daltons, in epithelial cells. The functional role of these proteins is still obscure but it seems likely that they may be involved in controlling the organization and distribution of organelles within the cytoplasm.

Microfilaments appear to be ubiquitous amongst the eukaryotic cells examined to date. They have a diameter of about 70 Å and can appear as stress fibres, like those in spread fibroblasts, or as bundles, which can be found in the microvilli of intestinal brush border cells (22, 23). These filaments are largely composed of polymerized actin, termed F-actin. The monomer, G-actin, is a globular protein with a molecular weight of 43,000 daltons which may account for 5-10% of the total protein in nonmuscle cells. Garrels and Gibson (24) have characterized three major isomers of actin which display slight differences in pI and can be found in varying ratios depending upon the cell type.

One form, α-actin, is found only in muscle cells, while nonmuscle cells have been shown to contain the β and γ forms. Muscle actin is probably the best understood of the three isomers but relatively little is known about the functional role of the β and γ forms.

In order to investigate cytoskeletal structures in detail it was convenient to select a cell type which was readily available and had a relatively stable structure. There are now two cytoskeletal models which have been thoroughly studied, both of which satisfied these two requirements. The microvillus structure of chicken intestinal brush border cells has provided the basis for one of the models. In general, these microvilli contain about 20 - 30 individual, closely packed microfilaments of 60 Å diameter. The filaments were identified on the basis of their general morphology and ability to bind heavy meromyosin. This protein binds specifically to actin in a manner which gives a characteristic array of arrowheads pointing in the same direction along the length of the filament (23, 25). By using this technique it was shown that the microfilaments were all polarized in the same direction and that they extended the full length of the microvillus. The distal ends were found to terminate in dense tip material, while the proximal ends were found to insert into the terminal web contained within the cell body. Further studies have shown that the microfilaments are held into a bundle by cross-linking molecules and that the bundle is attached to the plasma membrane by lateral arms (26). The microfilament-membrane attachment in the region of the lateral arms is clearly different from that in the dense tip material, although the exact structural variations are still unclear. In fact, little is known about the exact method of attachment in either region. Early studies seemed to suggest that

α-actinin might be involved in the membrane attachment, particularly at the tips, but this is now strongly disputed (27-29).

Isolated brush border microvilli can be 'demembranated' by Triton X-100 extraction to leave behind the insoluble, microvillar core structure (30). Sodium dodecyl sulfate polyacrylamide gel electrophoresis shows that this material contains four major polypeptides with molecular weights of 110,000, 95,000, 68,000 and 42,000 daltons. Matsudaira and Burgess (30) combined biochemical investigations with electron microscopy studies to try to determine which of these components may provide the lateral arms and cross-links. When the microvillar cores were treated with ATP and Mg^{2+} they observed that the microfilaments remained cross-linked while there was a disappearance of the lateral arms. This was accompanied by a decrease in the quantity of the 110 K protein. However, when the cores were incubated with deoxycholate the lateral arms remained, the cross-links disappeared and there was a reduction in the quantity of the 95 K and 68 K components. These results provide evidence that the 110 K component may be directly or indirectly attaching the microfilament bundle to the membrane. Unfortunately there is insufficient data to be able to determine whether either or both of the lower molecular weight proteins may be cross-linking the actin filaments. Other studies have shown that the 95 K protein (villin) is capable of bundling F-actin <u>in vitro</u> to produce structures similar in morphology to the microvillar bundles (31, 32). The 68 K protein called fimbrin has been detected in a variety of different cells. It is present in regions of highly ordered microfilaments and in membrane ruffles which contain a fine microfilamentous network (33). This diverse distribution has offered few clues

to its functional role.

In the electron microscope membranes appear to have a trilaminar, railroad track image produced by the method of fixation and staining. When the intestinal brush border microvilli are treated with nonionic detergent the membrane is solubilized and no peripheral trilaminar structure can be observed. This effect is not necessarily a general phenomenon. Mescher, Jose and Balk (34) have examined the Nonidet P-40 insoluble material from the plasma membranes of murine ascites tumor cells. They observed a residual matrix which contained actin as a major component. It was suggested that this structure may serve to stabilize the lipid bilayer and mediate the interaction of transmembrane proteins with the cytoskeleton.

Red blood cells have provided the second and arguably the best understood of the two major cytoskeletal models. Erythrocyte membranes can be prepared simply by lysing the cells with hypotonic shock. This releases the cell contents and leaves the membrane in an open 'ghost' structure (35). Since red blood cells have no internal membranes ghost preparations are very pure. They also have an additional advantage in that both sides of the membrane can be studied with equal facility.

The erythrocyte cytoskeleton, again defined as that material which is insoluble in Triton X-100, contains spectrin as its major component. This protein is composed of similar but not identical subunits, with molecular weights of 240,000 and 220,000 daltons (36). These are called band 1 and band 2 in the nomenclature of Fairbanks et al. (37). The rest of the triton-insoluble material consists of band 3 (actin), band 2•1 (ankyrin), band 4•1, some band 3 and several other minor components.

Shotton et al. (38) used platinum-carbon replicas produced by low angle shadowing to observe the spectrin heterodimer. They found it to be a flexible rod about 1000 Å long composed of two strands twisted around each other. The dimers were also found to have an end to end association, thereby forming a tetramer in the native membrane. More recently Goodman and Weidner (39) have isolated a spectrin tetramer in low ionic strength solutions at 4°C which they propose is the usual form of spectrin in the intact cell. Ungewickell et al. (40) and Cohen et al. (41) also propose that spectrin is a tetramer in the native state and that it can form a filamentous network when associated with actin and band 4•1. Since each spectrin dimer has one actin binding site the cross-linking usually found in these complexes can only be achieved by the tetramer. When isolated spectrin and band 4•1 are mixed with F-actin cross-linking and gelation occur. If the actin is in the monomeric form there is no gelation. This implies that the actin associated with erythrocyte membranes must be in a polymerized form. However, electron microscopy studies have been unable to detect any actin microfilaments associated with the membranes or in the Triton residues. Instead, the cytoskeleton appears as an irregular network of small, anastomosing filaments with globular projections (42). It has been postulated that the F-actin is in short pieces called oligomers but there is no unequivocal evidence in support of this proposal.

Erythrocyte membranes can be induced to form spectrin-depleted, inside-out vesicles, so exposing many high affinity spectrin binding sites (43). When these inside-out vesicles are treated with chymotrypsin the spectrin binding activity is lost and a protein of 72,000

daltons is released into the surrounding medium (44). Antibody against this protein cross-reacts with band 2•1, suggesting that this protein may be involved at the spectrin-membrane binding site (43). Furthermore, peptide maps of 72 K and band 2•1 appear to be identical (46, 47). Detergent extraction of spectrin-depleted vesicles solubilizes a complex containing band 3 and band 2•1 (48). In addition band 3 has been shown to span the lipid bilayer. It is therefore probable that ankyrin is a linking protein between spectrin and the integral membrane protein band 3. This type of complex provides a mechanism whereby the cytoskeleton could influence, or be influenced by, the external surface of the plasma membrane.

The cell surface molecules of erythrocytes are relatively immobile. It is therefore surprising that only 10-20% of the band 3 molecules appear to be associated with ankyrin. In general, it is thought that the cytoskeleton may be involved in controlling the mobility of any surface components which are 'tied' to it. In this case the cytoskeleton appears to restrict the movement of only a small proportion of surface proteins. These anchored components may act to indirectly impede the movement of the other 'free' components.

The cytoskeletal structures of intestinal brush border microvilli and red blood cells have been intensively investigated and detailed cytoskeketal models have been proposed. However, it is unlikely that these models can be directly extrapolated to other systems as they are based on cells which are highly differentiated in both structure and function. Further studies using less specialized cells may yield information which is more generally applicable.

The cells used to carry out the research described in this thesis

were the stable B1 and C1 sublines of the 13762 rat mammary adenocarcinoma. The original solid tumor was chemically induced by dimethylbenzanthrene in a normal rat mammary gland. This form was then converted into three distinct ascites lines, MAT-A, MAT-B and MAT-C, at the Mason Research Laboratories. While these lines were being carried at Oklahoma State University the MAT-B1 and MAT-C1 sublines were developed as derivatives of the MAT-B and MAT-C cell lines. These are now maintained by weekly passage through the peritoneal cavity of female rats (49).

Initial investigations revealed that the MAT-C1 cells are xenotransplantable whereas the MAT-B1 cells are not (50). In addition the sublines also display several other differences, including very distinct morphologies. Scanning electron microscopy has shown that the MAT-C1 cells have a dense covering of highly branched microvilli, while the MAT-B1 cells are covered with straight microvilli (51). Further studies revealed that the concanavalin A receptors of the MAT-C1 cells do not appear to undergo redistribution in the presence of the lectin even when the cells are treated with cytochalasin B, colchicine or hypotonic buffers. Furthermore, these treatments do not cause disruption of microvillar structure, although they do enhance microvillar shedding. In contrast MAT-B1 cells have highly mobile concanavalin A receptors. Moreover, treating these cells with cytochalasins for example can cause gross changes in cellular morphology, including disappearance of microvilli (49). It has been suggested that MAT-C1 microvilli have a highly stabilized cytoskeleton. Hence, the restricted mobility of the concanavalin A receptors could be caused by their transmembrane interactions with this stabilized sub-structure.

In order to investigate possible differences in protein composition MAT-B1 and MAT-C1 microvilli were compared by polyacrylamide gel electrophoresis (52). The major difference was found to be the presence of a 58,000 dalton polypeptide (58 K) in MAT-C1 microvilli which was greatly reduced or absent in MAT-B1 microvilli. Subsequent observations showed 58 K to be insoluble in Triton X-100. However, this protein was also found to be associated with microvillar membranes (MF2) produced from microvilli by hypotonic swelling, followed by homogenization and differential centrifugation. 58 K therefore appears to be directly or indirectly associated with the plasma membrane and the cytoskeleton. It has been postulated that this protein may play a role in stabilizing the cytoskeleton of these microvilli. If this is the case it may also have some restrictive influence over the mobility of the surface lectin receptors.

In addition to 58 K the MF2 vesicles also contain actin as a major component, although no recognizable microfilaments can be observed by electron microscopy. Gel filtration studies have indicated that this actin is of a size intermediate between that of F and G, and probably represents an oligomeric form (53).

Previous investigations using these cell lines employed the technique of transmission electron microscopy to make some basic morphological observations and to check the purity of particular preparations. The aim of this research was to carry out a comparative ultrastructural characterization of microvilli, membranes and cytoskeletal residues derived from the MAT-B1 and MAT-C1 cells. Transmission electron microscopy was combined with biochemical techniques in order to correlate protein composition with morphological structures.

CHAPTER II

METHODS

Preparation of Cells

The MAT-B1 and MAT-C1 sublines of the 13762 rat mammary adenocarcinoma were maintained by weekly intraperitoneal injection of cells into female rats, as previously described (49). After 6 days the cells were gently aspirated from the peritoneal cavity and washed three times by resuspension in PBS-Mg^{2+}-glucose (120 mM NaCl, 5 mM KCl, 20 mM Na_2HPO_4, 2 mM NaH_2PO_4, pH 7.4, containing 2 mM $MgCl_2$ and 0.1% w/v glucose) and centrifugation at 75 x g for 5 minutes. Cells to be used for IEF-SDS PAGE or electron microscopy were washed three times by resuspension in PBS-Mg^{2+}-glucose and centrifugation at 1000 rpm for 5 minutes in a Sorvall Instruments GLC-4 general laboratory centrifuge.

In some experiments cells were metabolically labeled. 15 μCi of [^{14}C]-glucosamine (in 0.3 ml of 0.9% w/v NaCl) were injected into the peritoneal cavity of a rat bearing MAT-B1 or MAT-C1 ascites cells. After 16 hours the cells were recovered by aspiration and resuspended in PBS-Mg^{2+}-glucose.

Preparation of Microvilli and Cell Bodies

Microvilli were prepared essentially by a previously described

protocol (54). The washed cells were incubated in PBS-Mg^{2+}-glucose containing 20% v/v calf serum, pH 7.4 (approximately 3 x 10^7 cells ml^{-1}), in a gyratory waterbath (New Brunswick Scientific Company Inc.) at 100 rpm and 37°C for 20-30 minutes. After this time the cells were gently drawn through a 14 gauge needle 10-14 times. The resulting suspension was centrifuged at 750 x g for 5 minutes to pellet the cell bodies. The supernatant fluid was removed and centrifuged at 40,000 x g for 30 minutes to produce a pellet of microvilli. This material was then resuspended in PBS-Mg^{2+} and washed twice.

Cell bodies to be used for IEF-SDS PAGE or electron microscopy were washed three times in the same manner as the whole cells.

Preparation of Microvillar Membranes

Microvillar membranes were prepared essentially using the method described by Cerra (54). Microvilli from the cells grown in two rats were resuspended in 12 ml GEM buffer to a protein concentration of approximately 0.3 mg^{-1}. The suspension was incubated at room temperature for 30 minutes and then homogenized (25 strokes) in a tight Dounce homogenizer. This was followed by centrifugation of the homogenate at 10,000 x g for 15 minutes. The supernatant fluid was removed and centrifuged at 100,000 x g and 4°C for 1 hour to collect the membrane fraction, MF2. In some experiments the procedure was modified by omitting the β-mercaptoethanol from the GEM buffer, thereby producing the fraction designated as MF. In other cases the 30 minute incubation was performed at 4°C, as specified in the figure legends.

Behavior of MF2 on a Sucrose Step Gradient

Microvillar membranes, MF2, were resuspended in GEM buffer to a protein concentration of approximately 200 μg ml^{-1}. 4 ml of this suspension was layered on top of a 4 ml sucrose cushion, 50% w/v in GEM buffer. This was centrifuged at 175,000 x g and 4°C for 16 hours. After this time the material which collected at the interface was recovered. It was diluted to 4 x its own volume with GEM and centrifuged at 100,000 x g and 4°C for 1 hour in order to pellet the membranes.

Triton X-100 Extraction of Microvilli and Membranes

Microvilli, MF, $MF2_c$ or MF2 (approximately 100 μg of protein ml^{-1} in the extraction medium, unless otherwise stated) were incubated in 0.2% v/v Triton X-100 in PBS containing 1 mM EGTA and 0.5 mM PMSF, pH 7.4, for 10 minutes at 37°C. The Triton-insoluble material was pelleted by centrifugation at 100,000 x g and 4°C for 1 hour. In some experiments the extraction of [^{14}C]-glucosamine label was followed by counting aliquots (usually 100 μl) of the extraction medium before and after the centrifugation step. Scintillation counting was carried out in a pre-mixed cocktail (Packard Insta-gel) using an LKB 1212 scintillation counter.

Dialysis

Triton X-100 supernatant fluids were dialyzed for 16 hours against three 1 liter changes of 0.1% w/v SDS, 1 mM EGTA, 0.5 mM

PMSF, 0.02% w/v sodium azide and 10 mM Tris, pH 7.4. The samples were then frozen, lyophilized and solubilized for 2D IEF-SDS PAGE.

Neuraminidase Treatment of Microvilli

Microvilli were resuspended in Dulbecco's PBS with 0.25 units of Vibrio cholerae neuraminidase activity ml^{-1} at 37°C for 30 minutes. The microvilli were then cooled to 4°C and centrifuged at 40,000 x g for 30 minutes (additional details, including definition of enzyme activity, in figure legend).

Determination of Protein Concentrations

Protein concentrations were determined by the method of Lowry et al. (55). BSA in the concentration range 20-200 μg ml^{-1} was used to construct the standard curves.

Sodium Dodecyl Sulfate Polyacrylamide Gel Electrophoresis

SDS PAGE was performed using the method previously described by Huggins et al. (49). Slab gels were generally 7.5% or 10% acrylamide, as specified in the figure legends.

2D Isoelectric Focusing-SDS PAGE

The methods employed were based on those of O'Farrell (56), as modified by Wilson et al. (57) and Leonardi and Rubin (58). Samples were solubilized by two procedures, in a total volume of 100-200 μl, using techniques described by Rubin and Leonardi (59).

Method 1: Stock grind (1% w/v SDS, 10% v/v β-mercaptoethanol, 9.5

M urea, pH 7.4), lysis supplement (10% v/v NP-40, 1.8% v/v 3-10 ampholines and 3.6% each of 4-6 and 5-7 ampholines) and lysis buffer (9.5 M urea, 2% v/v NP-40, 0.4% v/v 3-10 ampholines and 0.8% v/v each of 4-6 and 5-7 ampholines) were added to the sample in the ratio 3:1:4 v/v.

Method 2: The sample was solubilized in one volume of solution A (2% w/v SDS, 5% v/v β-mercaptoethanol, 60 mM Tris-HCl, pH 6.8) and two volumes of solution B (9.5 M urea, 5% v/v β-mercaptoethanol, 8% v/v NP-40, 0.4% v/v 3-10 ampholines and 0.8% v/v each of 4-6 and 5-7 ampholines).

Isoelectric focusing tube gels (0.3 cm x 11 cm) were prepared as described by O'Farrell (56) except that the acrylamide concentration was reduced to 3%. In addition the ampholines concentration was increased to 6% by volume and consisted of Biorad ampholines pH 3-10, 4-6 and 5-7 in a ratio of 1:2:2 (58). The gels were prerun at a constant current and the voltage was allowed to rise continuously from 175 volts to 400 volts. At this point the pre-run was stopped, the samples were applied and run for 19 hours at 400 volts. After completing the run the gels were removed from the tubes and the pH gradient was periodically checked using a Micro combination pH probe (Microelectrodes Inc.). The gels were then incubated at 25°C for 30 minutes in sample buffer (10% v/v glycerol, 5% v/v β-mercaptoethanol, 2% w/v SDS and 0.0625 M Tris-HCl, pH 6.8). After this step the tube gels were transferred to the second dimension slab gels (10% acrylamide separating gel) and anchored in place using 1% w/v agarose in hot sample buffer containing 0.002% w/v bromophenol blue. Upon cooling the second dimension was run at a constant current of 20 mA.

Silver Staining Slab Gels

Slab gels were silver stained by the method of Goldman et al. (60). In some cases gels were first stained with Biorad Coomassie brilliant blue R-250, destained and then silver stained. The first step of the procedure required the gel to be soaked in 50% methanol and 12% acetic acid, for a minimum of 20 minutes. This was followed by three 10 minute washes in 10% ethanol and 5% acetic acid with continuous agitation. The gel was then soaked in 0.0034 M potassium dichromate and 0.0032 N nitric acid for 5 minutes. This solution was aspirated and four rapid distilled water washes followed. The gel was next immersed in 0.012 M silver nitrate for 30 minutes with gentle shaking. The first 5 minutes of this incubation were in the presence of a fluorescent light source. Immediately after the removal of the silver nitrate solution the gel was rapidly rinsed, at least twice, in about 200 ml of image developer. This consisted of 0.28 M sodium carbonate and 0.05% formalin. The gel was gently agitated in fresh image developer until it reached the desired intensity. At this time the developing solution was replaced by 1% acetic acid solution.

Electron Microscopy Techniques

Samples were routinely fixed in 2% glutaraldehyde and 0.2% tannic acid for 1 hour, followed by postfixation in 1% osmium tetroxide for 30 minutes. These operations were carried out at room temperature in 50 mM sodium cacodylate buffer, pH 7.2. Whole cells were fixed in 3% glutaraldehyde for 1 hour and postfixed in 1% osmium tetroxide for 30 minutes. In this case 50 mM Sorensen's phosphate buffer, pH 7.2, was

used throughout at room temperature (61). The fixed samples were dehydrated in an ethanol-propyleneoxide series and embedded in Araldite 502. Thin sections were cut with glass knives, mounted on copper grids and counterstained with 2.5% w/v uranyl acetate in 50% v/v ethanol and 2.7% w/v lead nitrate with 3.5% w/v sodium citrate dihydrate.

Negative staining was carried out by applying 10 µl of sample suspension to a formvar and carbon-coated copper grid for 10-15 seconds. The grid was then washed with 4 drops of 1 mg ml^{-1} cytochrome c; 4 drops of distilled water; and 4 drops of a 1:20 dilution of a saturated uranyl acetate solution. The grids were then allowed to air-dry. Negatively stained material and thin sections were observed at 60 KV in a Philips 300 electron microscope.

Light Microscopy Techniques

Cells were fixed and embedded as described in the previous section. Thick sections (0.75 µm) were cut using glass knives and mounted on a glass slide. The sections were incubated in 0.5% w/v periodic acid for 10 minutes at 65°C, after which they were washed with distilled water. Schiff reagent (Fisher Scientific Company) was then applied to the sections for 5 minutes at 65°C, followed by a second distilled water wash. Total evaporation of the warm solutions was avoided by replenishing the liquid as required. Following this the sections were dried, lightly counterstained with toluidine blue (0.1% w/v toluidine blue, 2% w/v sodium bicarbonate in distilled water) and redried. This method is essentially that described by Di Bella and Hashimoto (62). The sections were then observed under an Olympus light microscope.

CHAPTER III

RESULTS

Ultrastructural Characterization of MAT-B1 and MAT-C1 Cells

Thin sections of Araldite embedded MAT-B1 and MAT-C1 cells were examined by transmission electron microscopy. The cells from both populations were heterogeneous in size, approximately 6-25 μm in diameter, and displayed several common characteristics (Figures 1 and 2). The rough endoplasmic reticulum was a prominent feature in both of the sublines. It was abundant throughout the cytoplasm and often had dilated cisternae. In many cases the cisternae appeared to contain fuzzy material which may represent newly synthesized protein destined for secretion, or incorporation into the plasma membrane. The cytoplasm contained large electron translucent areas which were identified as lipid droplets on the basis of their morphology. In addition, darkly staining 'rosettes' were localized in discrete areas throughout the cytoplasm. The morphology and distribution of this material suggested that it might be glycogen. In order to test this possibility araldite embedded cells were cut into thick sections, stained with PAS and Toluidine blue and examined under a light microscope. Using the conditions previously described PAS stains carbohydrate pink, while Toluidine blue stains nuclei deep blue and

Figure 1. High Magnification Transmission Electron Micrographs of MAT-B1 and MAT-C1 Cells.

A) MAT-B1 cell, B) MAT-C1 cell. Magnifications: A) and B) 18,500 X. Bars = 1 μm.
G = glycogen, G_O = golgi, L = lipid, M = mitochondria, Mv = microvilli, N = nucleus, RER = rough endoplasmic reticulum.

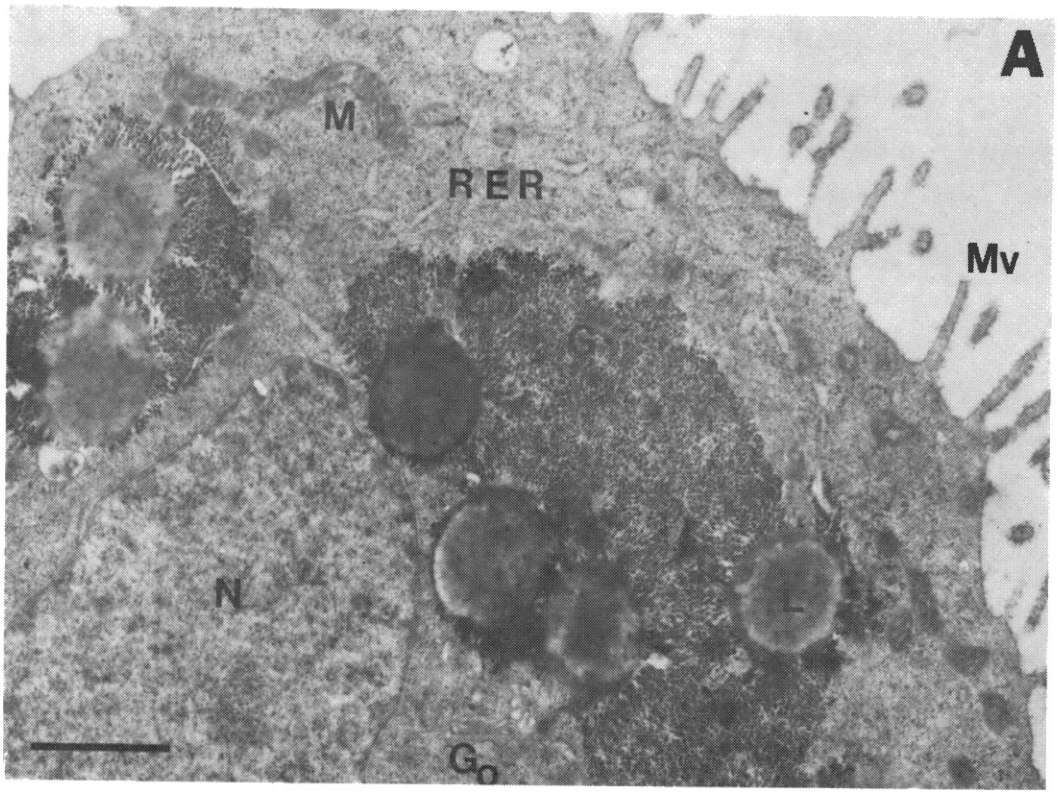
A
M
RER
Mv
N
L
G_0

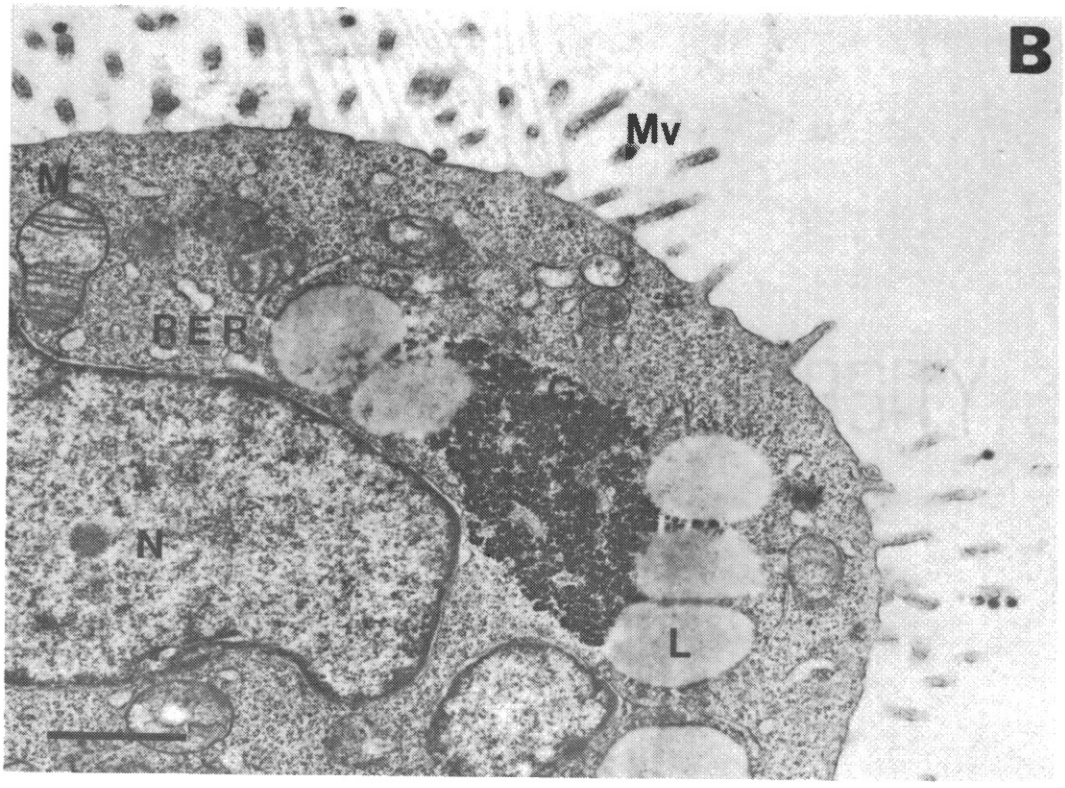
B
Mv
M
RER
N
L

Figure 2. Transmission Electron Micrographs of MAT-B1 and MAT-C1 Cells and Microvilli.

A) MAT-B1 cell, B) MAT-C1 cell, C) MAT-C1 cell, D) MAT-B1 microvilli, E) MAT-C1 branched microvillus, F) MAT-C1 microvilli, G) MAT-C1 microvilli and viruses. Magnifications: A), B) and C) 5,500 X; D), E), and F) 28,000 X; G) 18,500 X. Bars = 1 μm.

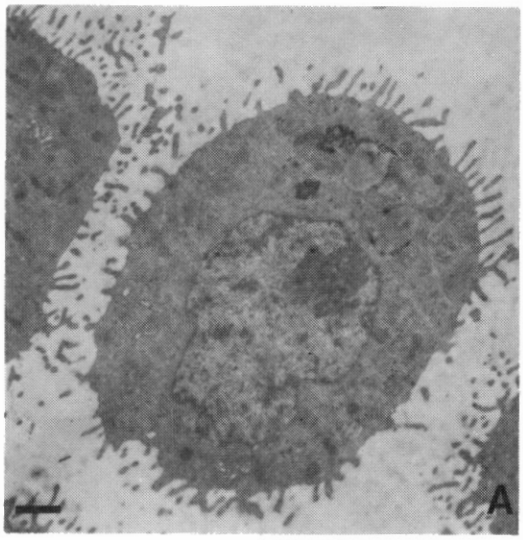
A

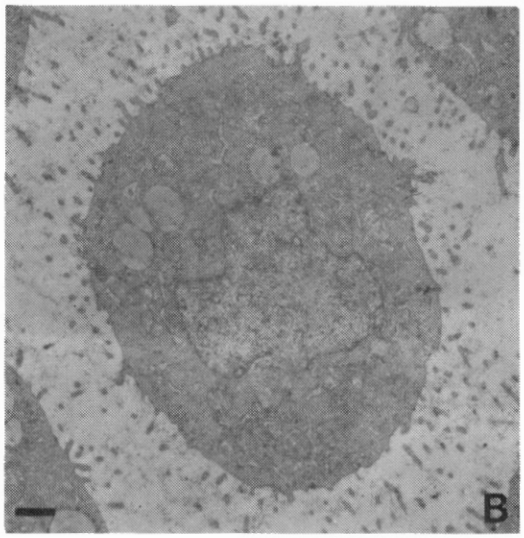
B

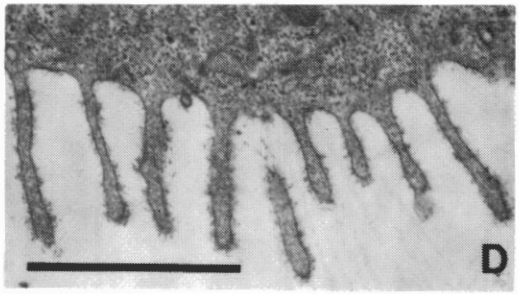
D

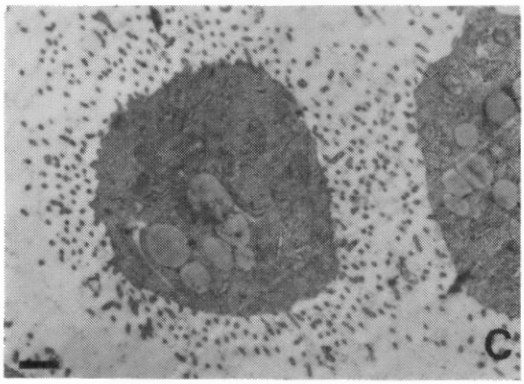
C

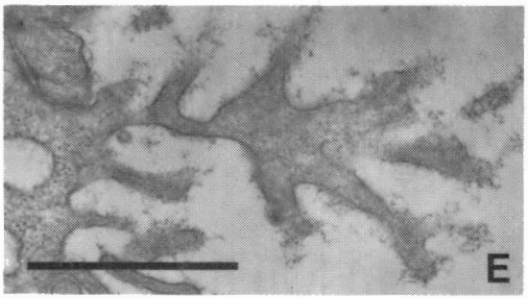
E

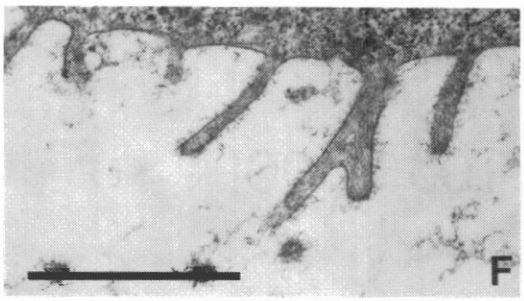
F

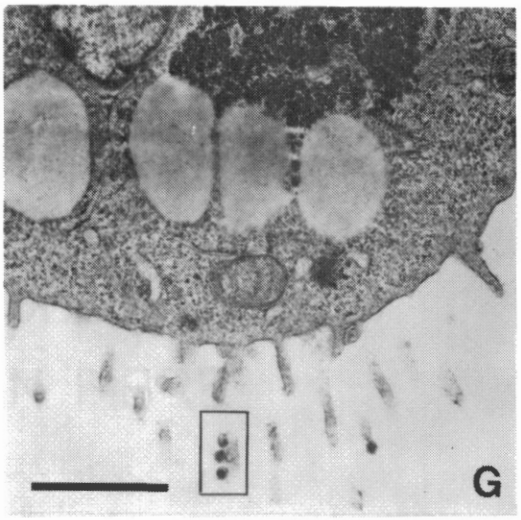
G

cytoplasm pale blue. Thus, it was shown that pink staining areas were present within the cells. These results combined with the TEM observations strongly suggest that both cell types contain large reserves of a carbohydrate which is probably glycogen.

The plasma membranes of the cells from both sublines were about 71 Å wide. Close examination of high magnification electron micrographs suggested that the membrane was asymmetrical with the outer leaflet being somewhat thicker than the inner leaflet. The external surfaces were covered by a layer of fuzzy material. This probably corresponds to the glycoprotein molecules which are known to be present in large quantities on the surface of these cells (50).

MAT-B1 and MAT-C1 cells displayed two major morphological differences. The most striking variation was the appearance of their mitochondria (Figure 1). These organelles were compact and darkly staining in the MAT-B1 subline. However, in the MAT-C1 cells they exhibited the typical orthodox form described by Hackenbrock (63) and were more lightly stained.

Scanning electron microscopy studies by Carraway et al. (51) demonstrated that MAT-B1 cells have many straight microvilli, while MAT-C1 cells have a dense covering of highly branched microvilli. In TEM the microvilli of MAT-B1 cells were found to be largely straight and 0.3-1.3 μm in length (Figure 2D). In contrast, the MAT-C1 cells were more usually surrounded by a dense halo of microvilli which were often cut in cross section (Figure 2C). Although some highly branched structures were observed very few of these were entirely within the plane of the section. Those which did appear to be in the same plane ranged from 0.4 - 2 μm in length (Figure 2E and 2F). In

both sublines the microvilli were generally 0.05 - 0.1 μm in diameter.

70 Å filaments were found within the cells of both sublines (these will be extensively discussed in following sections). Intermediate filaments and microtubules were rarely detected in either MAT-B1 or MAT-C1 cells.

After whole cells were sheared to remove microvilli the cell bodies were examined by TEM. Many seemed to be unaffected by this process, while others appeared to have a reduced number of microvilli, at least within the plane of the section. However, some regions of the plasma membrane were entirely devoid of microvilli (Figure 5C and 5F). In these areas distinct breaks in the continuity of the membrane could be distinguished which may represent the sites of microvillar detachment.

Many electron opaque particles were present amongst the MAT-B1 and MAT-C1 cells (Figure 2G). The particles outside the cells were approximately 700 - 1000 Å in diameter and consisted of a densely staining, circular or C-shaped structure, surrounded by a membrane, or envelope, which had fuzzy material covering the external surface. In many cases the darkly staining material was off-center with respect to the middle of the area enclosed by the membrane. Inside the cells circular structures were observed, within the cytoplasm, which appeared to be similar to those inside the extracellular particles. In some cases the darkly staining circles could be seen immediately below the plasma membrane, which appeared to be enclosing them and pinching off from the rest of the cell. The particles were frequently found adjacent to the microvilli, and on occasions their membranes appeared to be continuous with the microvillar membrane, as already described.

This morphology is comparable to that of the RNA containing mouse mammary tumor virus (64). Although the particles in the MAT-B1 and MAT-C1 preparations had a very similar morphology, they may or may not have been the same in terms of their molecular composition.

2D IEF-SDS PAGE Analysis of Whole Cells and Cell Bodies

The 2D IEF-SDS PAGE patterns obtained from whole cells and cell bodies were very complex (Figure 4). However, they do demonstrate the great resolving power of this technique. The pH gradient across the gels was linear over the range pH 7•2 to pH 4•4, as illustrated in Figure 3. All the 2D gels are arranged so that the basic regions are on the left and the acidic regions are on the right.

Earlier studies using 1D SDS PAGE demonstrated that there was no significant difference in the major polypeptides present in the whole cells and cell bodies from either subline (C. A. C. Carraway, unpublished observations). 2D gel patterns obtained for the MAT-B1 preparations strongly supported the previous findings (Figure 4A and 4B). There was near complete homology in the gel patterns of the whole cells and cell bodies. This finding might be expected since the production of cell bodies from whole cells seems to involve the removal of only a small number of the total available microvilli, which probably represent only a very small fraction of the total cellular protein. The data for the MAT-C1 preparations was less clear cut as the gel of the whole cell protein composition was somewhat underloaded for Coomassie blue staining (Figure 4C). However, 29 of the polypeptide spots detected in the gel of whole cells were

Figure 3. 2D IEF-SDS PAGE Pattern for MAT-B1 Whole Cells, Showing pH Gradient and Molecular Weight Markers.

A) MAT-B1 whole cells, gel stained with Coomassie blue, B) pH gradient across the gel. Bars indicate molecular weight markers, from top to bottom: 68,000 daltons, 43,000 daltons and 30,000 daltons.

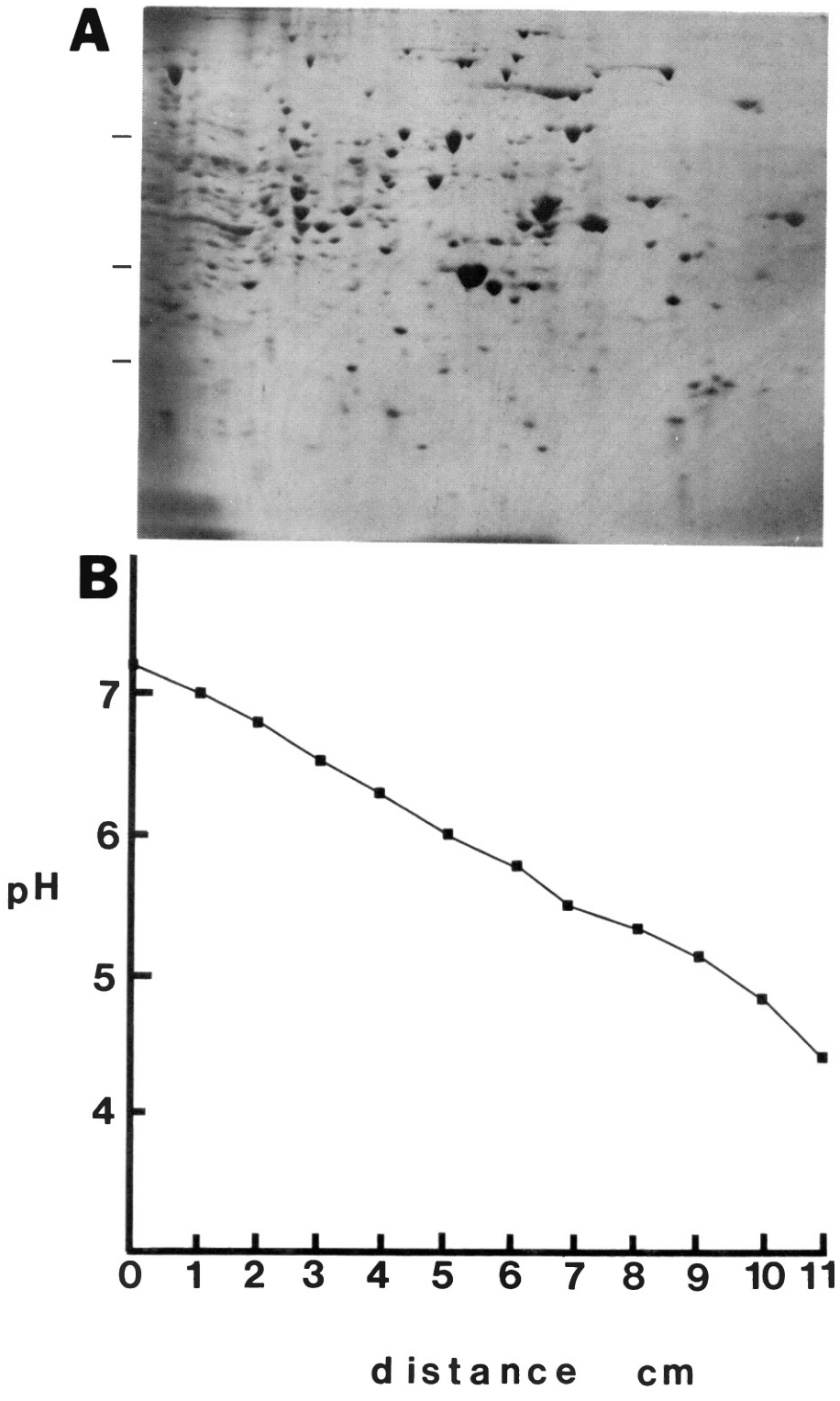
A
B
7
6
5
4
pH
0 1 2 3 4 5 6 7 8 9 10 11
distance cm

Figure 4. 2D IEF-SDS PAGE Analysis of MAT-B1 and MAT-C1 Whole Cells and Cell Bodies.

A) MAT-B1 whole cells, B) MAT-B1 cell bodies, C) MAT-C1 whole cells, D) MAT-C1 cell bodies. All gels stained with Coomassie blue.

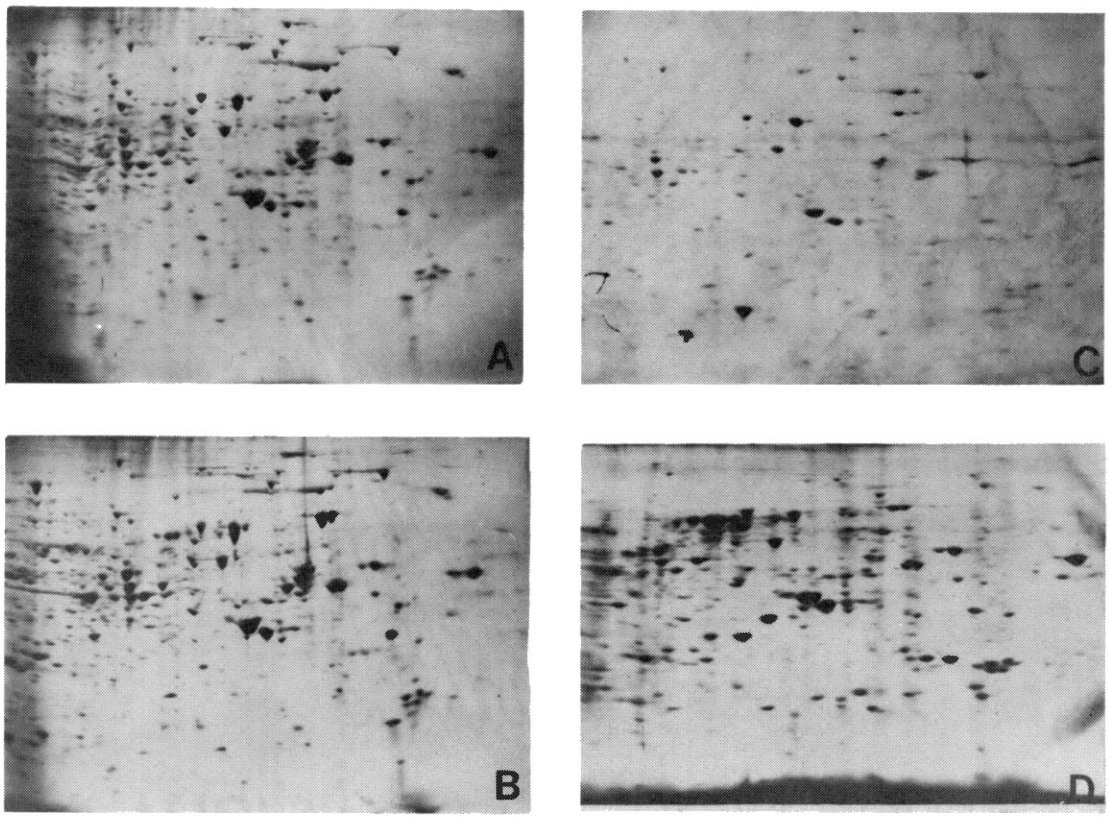
A
C
B
D

also present in the cell bodies (Figure 4D).

Ultrastructural Characterization of Microvilli and Microvilli Preparations

Electron microscopy observations revealed that the microvilli extending from the cells of both sublines contained filaments of approximately 70 Å in diameter (Figure 2D, 2E and 2F). Actin is known to be a major component of the isolated microvilli from both sublines (54, 65). This information combined with the morphological observations strongly suggests that the 70 Å filaments are actin microfilaments.

Examination of microvilli attached to intact MAT-B1 and MAT-C1 cells showed that the microfilaments ran parallel to the long axis, but did not extend the full length of each microvillus. Where the ends of the microfilaments were visible they curved in towards the membrane, at the proximal and distal ends. The microfilaments may have been attached to the membrane in these regions but it was not possible to verify this proposal from these observations. In the areas where each microvillus was attached to the cell body the microfilaments began to spread out and merge into the cytoplasm. They did not appear to terminate in any kind of organized structure. In fact there were no structures comparable in morphology to the dense tip material or terminal web found in the microvilli of intestinal brush border cells (66).

After shearing and sequential differential centrifugation microvilli or microvillar fragments (approximately 0.2 - 1.3 μm long and 0.05 - 0.1 μm wide) were observed in which the filaments were preserved

essentially intact (Figure 5). Cross-sections of attached and isolated microvilli showed that the microfilaments were distributed throughout the interior of each microvillus. However, they did not seem to be organized into a regular array.

In MAT-B1 and MAT-C1 preparations many fragments were observed which had a membranous vesicle at one end. These structures probably represent the positions where the microvilli were pulled away from the body of the cell. Shearing must break the plasma membranes in order to release the microvilli. The ruptured membrane at the base of each fragment may then reseal and vesiculate in order to achieve a more thermodynamically stable structure. Microvillar fractions produced by the techniques employed here appeared to be contaminated by membrane vesicles which were not attached to microvilli. However, it is probable that they were in fact attached to microvilli which extended out of the plane of the section. The vesicles observed in MAT-B1 preparations often had two microvillar fragments attached to them (Figure 5A). These structures were greatly reduced in amount or absent from the MAT-C1 preparations.

Many boomerang shaped fragments were present in MAT-C1 microvillar fractions which were generally absent from the MAT-B1 preparations (Figure 5D). These structures probably represent an oblique cut through the branched part of a microvillus. The curved sections often had one or more bulbous protrusions along their length, which may correspond to sites where the fragment was detached from the rest of the microvillus. Alternatively, the protrusions may be tangential sections through branches which extend out of the plane of the section.

The external surfaces of the microvillar and vesicle membranes

Figure 5. Transmission Electron Micrographs of MAT-B1 and MAT-C1 Microvilli and Cell Bodies.

A) and B) MAT-B1 microvilli, C) MAT-B1 cell body, D) and E) MAT-C1 microvilli, F) MAT-C1 cell body. Magnifications: A) and D) 47,000 X; B) and E) 82,000 X; C) and F) 26,500 X. Bars = 0.5 μm.

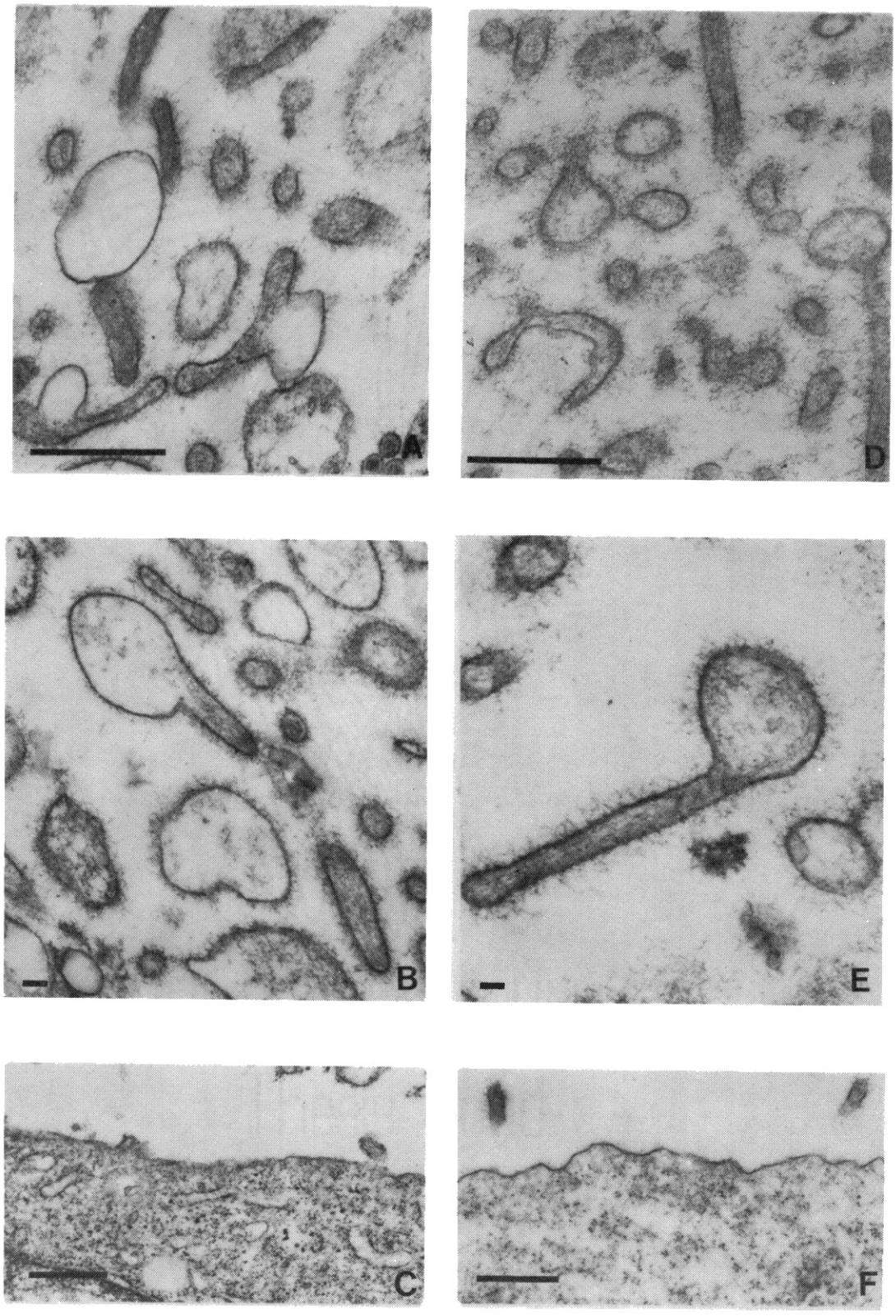
A
D
B
E
C
F

were covered in a dense layer of fuzzy material which probably corresponds to the glycocalyx. In addition, the vesicles also had amorphous material on their inner surfaces. This may be of cytoskeletal origin or it may represent residual cytoplasmic components which became trapped within the vesicles during the shearing process.

Microvillar fractions derived from both MAT sublines were significantly contaminated by the putative viral particles described earlier.

2D IEF-SDS PAGE Analysis of MAT-B1 and MAT-C1 Microvilli Preparations

2D IEF-SDS PAGE patterns for the microvillar fractions were considerably less complex than those obtained for whole cells (Figures 6 and 7). Previous research demonstrated that actin was a major component of the MAT-B1 and MAT-C1 microvilli, while this technique revealed that actin was present as a characteristic double spot with two pI values. The two types probably correspond to the β and γ isomers which are generally regarded as nonmuscle forms (24). This proposal was supported in part by the fact that neither of these spots migrated in the same position as skeletal muscle α-actin.

A triplet of spots with an apparent molecular weight of approximately 30,000 daltons and a pI in the region of pH 5 was present in the microvillar fractions from both sublines (Figures 6 and 7). It was reasoned that a pair of these spots might represent the subunits of nonmuscle tropomyosin. In order to test this possibility solubilized microvilli were run on 2D gels with purified skeletal muscle tropomyosin. The standard had a similar pI but a slightly higher molecular weight

Figure 6. 2D IEF-SDS PAGE Analysis of MAT-C1 Microvilli.

A) MAT-C1 microvilli, gel stained with Coomassie blue, B) MAT-C1 microvilli, gel silver stained. pH range 7.2 - 4.4. 1_b = β-actin, 1_c = γ-actin, 2 = 58 K, 3 = CAG, 4 = ASGP-2.

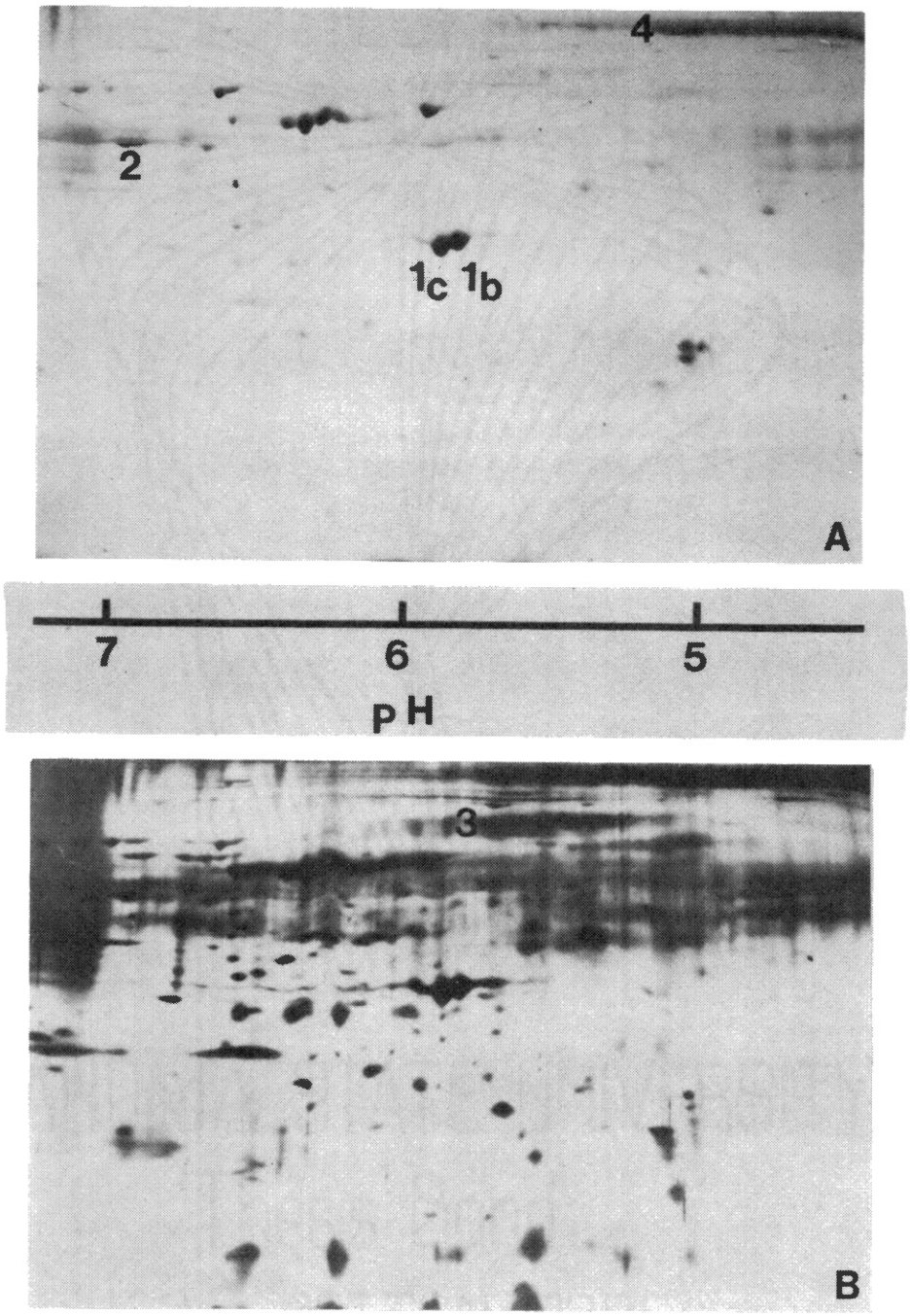
4
2
1c 1b
A
7
6
5
pH
3
B

Figure 7. 2D IEF-SDS PAGE Analysis of MAT-B1 Microvilli and Microvilli Treated with Neuraminidase.

A) MAT-B1 microvilli incubated in DPBS for 30 minutes at 4°C, B) MAT-B1 microvilli incubated in DPBS for 30 minutes at 37°C, C) MAT-B1 microvilli incubated in DPBS for 30 minutes at 37°C with 0.25 units of neuraminidase activity ml^{-1}. All gels silver stained.
One unit of enzyme activity is defined as the amount of enzyme that will release 1 μM of N-acetylneuraminic acid from human acid α_1-glycoprotein per minute at 37°C in 0.05 M sodium acetate buffer, pH 5.5, containing calcium chloride, 1 mM, and Haemaccel, 1.75 grams per liter.

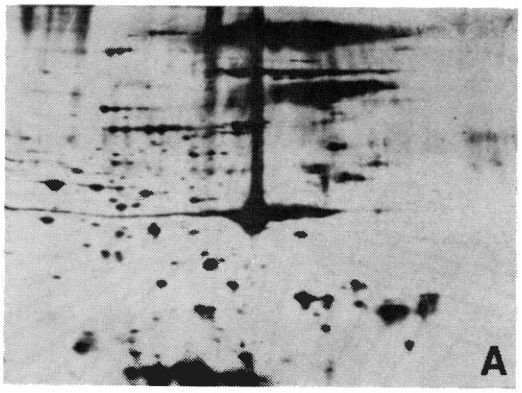
A

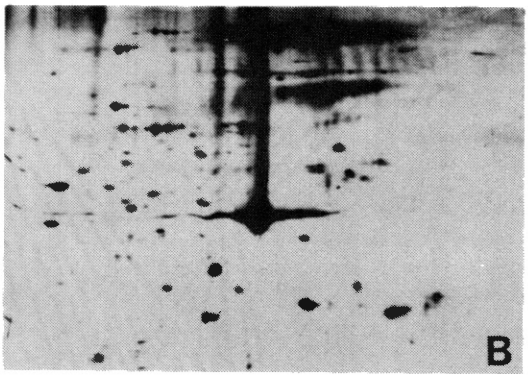
B

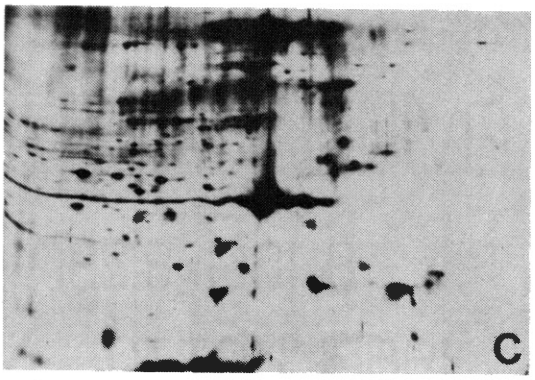
C

than the spots which comprise the triplet. This data alone is inconclusive since molecular weight differences between muscle and nonmuscle tropomyosins were documented by Korn in 1978 (67). In a companion study MAT-C1 cells were fixed, permeabilized and incubated with affinity purified antibody against skeletal muscle tropomyosin. After several washes an antibody sandwich technique was used to attach a fluorescent tag to any of the antitropomyosin which remained in the cells. No fluorescence above background levels was localized within the microvilli, which therefore indicated a lack of tropomyosin in these structures (R. H. Warren, unpublished observations). However, the possibility remains that the microvilli contain a form of nonmuscle tropomyosin which is unable to cross-react with the antibody against skeletal muscle tropomyosin.

Previous studies have shown that the MAT-C1 microvilli contain a 58,000 dalton polypeptide which is reduced in amount or absent in MAT-B1 microvilli (52). On 2D gels 58 K had a pI at approximately pH 6.8 but it was difficult to obtain an accurate value as this component had a tendency to smear across the gel (Figure 6). Horizontal streaks frequently occur when proteins are not fully solubilized as this prevents them from focusing properly in the first dimension IEF (68). This technique also showed that 58 K had a shadow band of slightly higher molecular weight which followed it in the IEF dimension.

A series of investigations by Carraway et al. (65) confirmed the presence of α-actinin in the microvilli isolated from MAT-C1 cells. A component with an apparent molecular weight of 100 K daltons, which may correspond to the α-actinin, was present on 2D gels of MAT-B1 and MAT-C1 microvilli. This polypeptide also smeared across the gels,

again reflecting incomplete solubilization.

Sialic acid containing glycoproteins have a characteristic appearance on 2D IEF-SDS PAGE. They leave an ascending trail of spots across the gel from a more basic to a more acidic pI. This phenomenon is caused by heterogeneous sialic acid content in the carbohydrate portions of these molecules. Increased or reduced amounts of sialic acid can alter the pI and apparent molecular weight of each molecule. If the gel is overloaded with respect to glycoprotein concentration the discrete spots coalesce to produce a broad band.

Gel patterns obtained for whole cells did not display any glycoprotein trails. This was expected since these molecules are relatively minor constituents of the total cellular protein. However, sialic acid containing glycoproteins are major components on the plasma membranes of MAT-B1 and MAT-C1 cells (69). It was therefore not surprising to find the distinctive trails when the microvillar fractions were analyzed on 2D gels (Figures 6 and 7). ASGP-1 is the most abundant sialic acid containing glycoprotein on both sublines. The second most abundant glycoprotein, ASGP-2, has a molecular weight of approximately 120,000 daltons and it had a low electrophoretic mobility in the second dimension molecular weight separation (69). This technique showed that the ASGP-2 molecules had pI's ranging from approximately pH 6 to pH 5 on MAT-B1 cells, and approximately pH 5•5 to pH 4•4, and possibly lower, on MAT-C1 cells.

2D gels of MAT-B1 microvilli had an additional trail of spots at an apparent molecular weight of approximately 65,000 daltons (Figure 7). This may have been another glycoprotein which was reduced in amount

or absent in the MAT-C1 microvilli but the 2D gel pattern alone is insufficient evidence upon which to base a firm conclusion.

The Coomassie blue stained 2D gels contained several other major and minor components in addition to those described above. In order to detect any further polypeptides these gels were destained and then silver stained. This procedure revealed another putative glycoprotein in both sublines with an apparent molecular weight of about 78,000 daltons (Figures 6 and 7). This component was barely visible by the previous staining method, which could be explained if 78 K was a minor component, or if it was unable to bind Coomassie blue as effectively as the other polypeptides in the gel. In previous studies using 1D gels 78 K went undetected because several other polypeptides which bind Coomassue blue heavily migrated in the same molecular weight region and masked its presence. In both sublines 78 K molecules had pI's in the range of approximately pH 6 to pH 5.

Although glycoproteins have a characteristic pattern on 2D gels it was desirable to provide some further evidence in support of their carbohydrate content. This was achieved by treating MAT-B1 microvilli with neuraminidase, to cleave off some of the sialic acid residues, and then analyzing the treated microvilli on 2D gels. The results of this experiment are shown in Figure 7. Two controls were performed by incubating microvilli at 4°C and 37°C without the enzyme to ensure that accelerated proteolysis at the higher temperature was not causing any major changes in the gel pattern. Neuraminidase treatment caused the glycoprotein spots to shift to more basic pI values. In addition, many of these spots shifted to positions of lower molecular weight. A change in the range of pI values might be expected if sialic residues

had been removed, as this would reduce the net negative charge on each glycoprotein molecule.

Previous studies have shown that MAT-B1 and MAT-C1 cells are able to incorporate [^{14}C]-glucosamine into ASGP-1 and ASGP-2 (69). It has now been demonstrated that this radio label is also metabolically incorporated into the 78 K component (Goeh Jung, unpublished observations), which provides further evidence to support the proposal that it is a glycoprotein.

Silver staining of 2D gels was a useful technique as it was able to detect very low concentrations of protein and stain 78 K. However, it did have one major disadvantage. This procedure enhanced two large horizontal streaks across the gel in the 50-60 K daltons molecular weight region. The streaks were eventually identified as impurities in the β-mercaptoethanol. Several commercially available sources of this chemical were tested in the IEF-SDS PAGE system but they all produced similar artifacts which were troublesome throughout this work.

Electron microscopy observations documented in the previous section described the presence of viruses in the microvilli preparations from both sublines. The identity of any polypeptides associated with the viruses remains to be determined.

2D IEF-SDS PAGE Analysis of MAT-B1 and MAT-C1 Microvillar Triton Residues

When membranes are extracted with Triton X-100 the insoluble material is generally regarded as being of cytoskeletal origin. The production of Triton extracted 'models' is now a standard technique

which has been used to assist the identification of cytoskeletal proteins in a number of systems (70). MAT-B1 and MAT-C1 microvilli were extracted with 0.2% Triton X-100 under conditions which are known to remove greater than 90% of [^{14}C]-glucosamine metabolically incorporated into MAT-C1 microvilli (C. A. C. Carraway, unpublished observations). 1 mM EGTA and 0.5 mM PMSF were included in order to minimize proteolysis. Triton-insoluble material was pelletable by centrifugation at 100,000 x g for 1 hour, so forming the Triton residue. The material which remained in the supernatant fluid after the centrifugation was defined as being Triton-soluble. Over 90% of [^{14}C]-glucosamine incorporated into MAT-C1 microvilli would remain in the supernatant fluid after centrifugation under these conditions. Triton-soluble and insoluble material was analyzed by 2D IEF-SDS PAGE.

The Triton residue from MAT-C1 microvilli contained three major components (Figure 8). Previous work demonstrated that actin and 58 K were insoluble in Triton X-100 but this analysis demonstrated that the β and γ isomers of actin were present and that 58 K was present along with its shadow band. The third constituent was the 78 K glycoprotein which was named CAG (cytoskeletal associated glycoprotein) because of its retention in the Triton residue. It is possible that this component may have merely co-sedimented with actin and 58 K during the centrifugation. However, recent studies by other researchers in our laboratory indicate that CAG can exist in a complex with actin and 58 K (Goeh Jung, unpublished observations). Preliminary studies employing DNase treatment and the myosin affinity technique also support the proposal that CAG may be associated with the cytoskeleton (C. A. C. Carraway, unpublished observations). Unlike CAG, the major cell surface glycoproteins

Figure 8. 2D IEF-SDS PAGE Analysis of MAT-C1 Microvilli, Triton-Insoluble and Triton-Soluble Components.

A) MAT-C1 microvilli, B) MAT-C1 microvilli Triton-soluble components, C) MAT-C1 microvillar Triton residue, D) MAT-C1 microvillar Triton Residue. A) and C) stained with Coomassie blue, B) and D) silver stained.

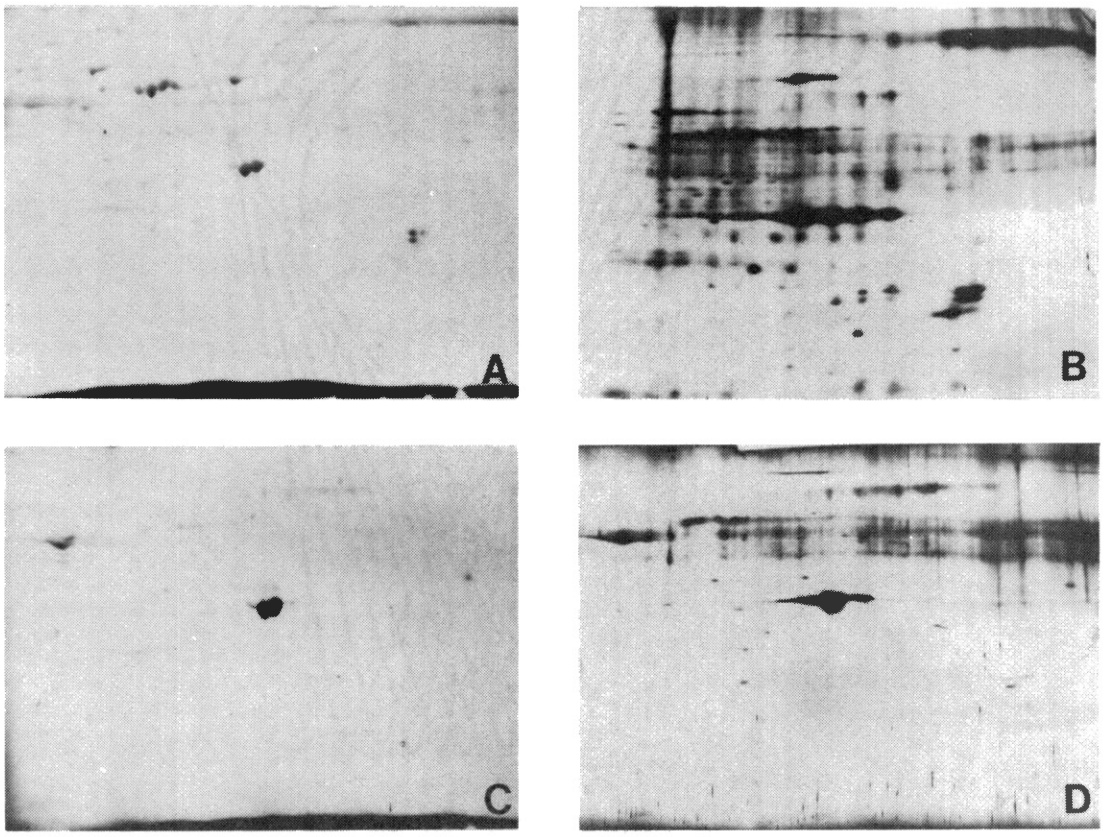
A
B
C
D

ASGP-1 and ASGP-2 are almost completely extracted by Triton X-100.

When sealed microvilli are iodinated using the ^{125}I-lactoperoxidase method ASGP-1, ASGP-2 and CAG become labeled (C. A. C. Carraway, unpublished observations), which suggests that CAG is exposed on the outside of the membrane. These results in conjunction with those already described imply that CAG is a transmembrane glycoprotein.

Actin and CAG were the only major components in the Triton residues derived from MAT-B1 microvilli (Figure 9). The 100 K dalton component, thought to be α-actinin, appeared to be present in the Triton-soluble and insoluble fractions from MAT-B1 and MAT-C1 microvilli. This may imply that it might interact, either directly or indirectly, with the cytoskeleton and the membrane.

Several other components were present in the Triton residues of both microvillar fractions. These polypeptides were only revealed by silver staining and were probably minor constituents. A few spots were present in the region of 60 K daltons on silver stained gels but it was difficult to determine whether they were constituents of the applied samples, or whether they were derived from the β-mercaptoethanol impurities.

The Triton-soluble material was dialyzed and lyophilized before being solubilized and applied to 2D gels. The resulting protein patterns were very difficult to interpret (Figure 8B) as this procedure causes individual polypeptides on the gel to appear as multiple spots with different pI's. Major components such as actin and ASGP-2 could be distinguished but the other components could not be reliably identified.

Figure 9. 2D IEF-SDS PAGE Analysis of MAT-B1 Microvilli and Microvillar Triton Residue.

A) MAT-B1 microvilli, B) MAT-B1 microvillar Triton residue, C) MAT-B1 microvillar Triton residue. A) and C) silver stained, B) stained with Coomassie blue.

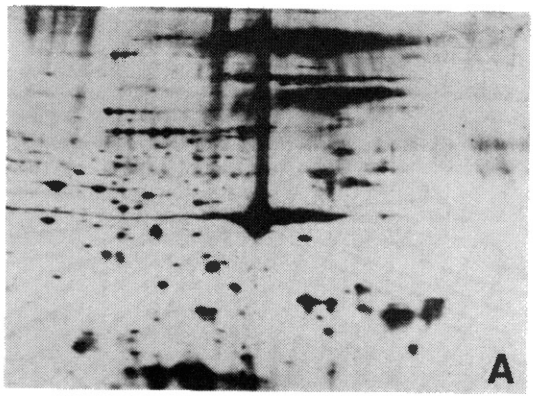
A

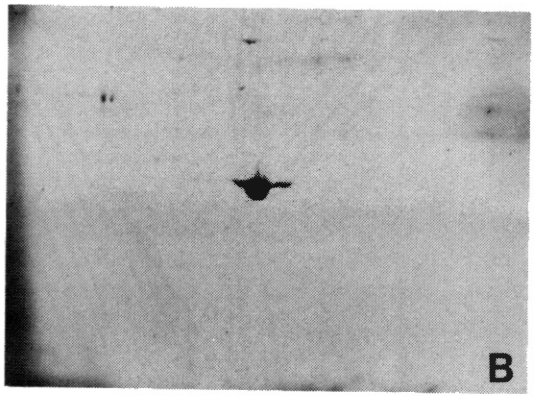
B

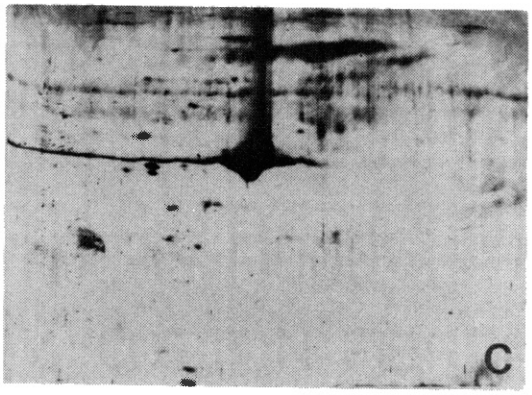
C

Ultrastructural Characterization of MAT-B1 and MAT-C1 Microvillar Triton Residues

The membrane glycoproteins of the MAT-B1 and MAT-C1 cells can be metabolically labeled with [^{14}C]-glucosamine, as previously described. In this laboratory the extraction of the radiolabel has been used to monitor the extent of glycoprotein extraction by Triton X-100, at total protein concentrations of 100 - 250 μg ml^{-1}. It was desirable to ascertain whether the extraction of the label could be correlated with the loss of membrane structure, as determined by the presence or absence of trilaminar images in samples examined by TEM. It was also of interest to find out whether actin filaments were preserved in the Triton-insoluble material.

MAT-B1 and MAT-C1 microvilli were extracted with Triton X-100 under conditions which are known to remove greater than 90% of the [^{14}C]-glucosamine label from MAT-C1 microvilli (C. A. C. Carraway, unpublished observations). The residual material was examined by negative staining and was shown to contain a mixture of filaments and vesicles (Figure 10). The filaments were approximately 70 Å wide, which is consistent with the morphology of microfilaments, and a number of them were branched. This image was not caused by the filaments simply crossing over, as close examination of high magnification pictures showed the continuity of the branches with the rest of the filament. The vesicles were heterogeneous in size (approximately 0.2 - 0.9 μm) and they appeared to be adhering to the fibrous material. It is possible that they represent incompletely extracted plasma membrane in association with Triton X-100 molecules. As such they may have remained attached to the filaments throughout, or they may have

Figure 10. Transmission Electron Micrographs of Negatively Stained MAT-B1 and MAT-C1 Microvillar Triton Residues.

A), B) and C) MAT-B1 microvillar Triton residues, D), E) and F) MAT-C1 microvillar Triton residues. Magnifications: A) and D) 16,300 X, B), C), E) and F) 25,500 X. Bars = 0.5 μm.

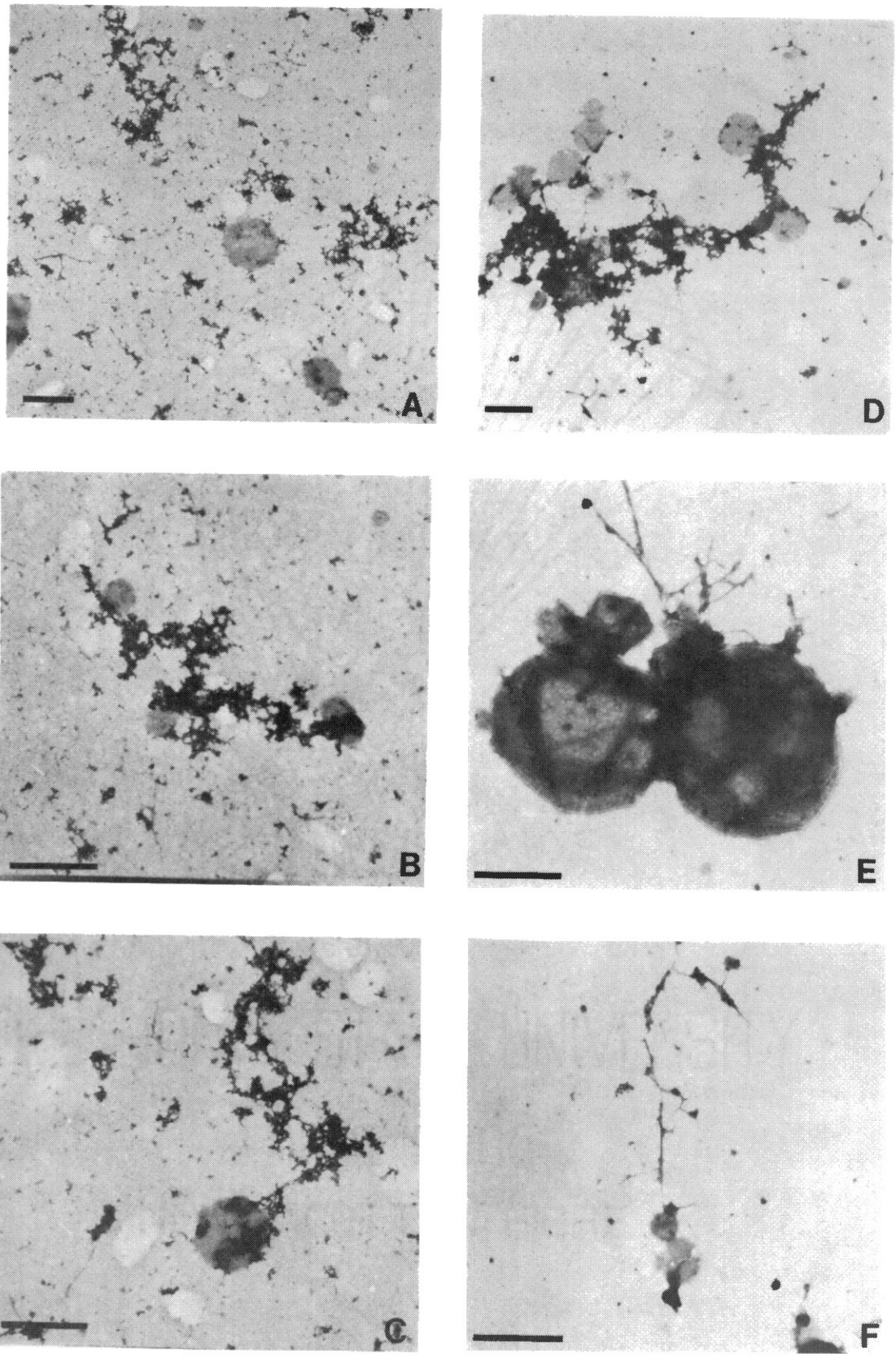
A
D
B
E
C
F

aggregated with the other material during the extraction and centrifugation. In many cases filaments could be traced across their surface and again these structures may be the remains of some in vivo structure or merely an aggregate.

TEM studies were also performed on thin sections. Triton X-100 extractions were carried out in parallel experiments on MAT-B1 and MAT-C1 microvilli. Both fractions were extracted at two protein concentrations, once at 100 - 150 $\mu g\ ml^{-1}$ and the second at a protein concentration of 4 X the first value. In all cases the extraction of metabolically incorporated [^{14}C]-glucosamine was measured (Figures 11 and 13).

The residues obtained from microvilli extracted at the higher protein concentration consisted of large sheets and vesicles, which had a trilaminar structure, interspersed with amorphous material (Figures 11A and 11B and 13A and 13B). Before extraction the plasma membranes were about 71 Å wide. After extraction the width of the trilaminar structures was considerably reduced and appeared to be in the range of 35 - 60 Å. There was a major difference in the morphology of the material at the top and bottom of each pellet. Amorphous material showed a greater concentration at the top of the pellet while the frequency of the trilaminar and multilamellar structures increased towards the bottom of the pellet.

At the lower protein concentration the Triton extracted residues seemed to have a more uniform morphology throughout (Figures 11C and 11D and 13C and 13D). The amorphous substance was still present but there were large areas of material which appeared to be filamentous. The dimensions of the filaments could not be determined as it was not

Figure 11. Transmission Electron Micrographs of MAT-B1 Microvillar Triton Residues.

MAT-B1 microvilli extracted with 0.2% Triton X-100 at a protein concentration of approximately:
I) 460 μg ml^{-1}. A) Top of the pellet, B) bottom of the pellet.
II) 115 μg ml^{-1}. C) Top of the pellet, D) bottom of the pellet.
Magnifications: A), B), C) and D) 52,500 X. Bars = 0.5 μm. The extraction of metabolically incorporated [^{14}C]-glucosamine was also determined. Amount of label extracted: I) 80.7%, II) 83.2%.

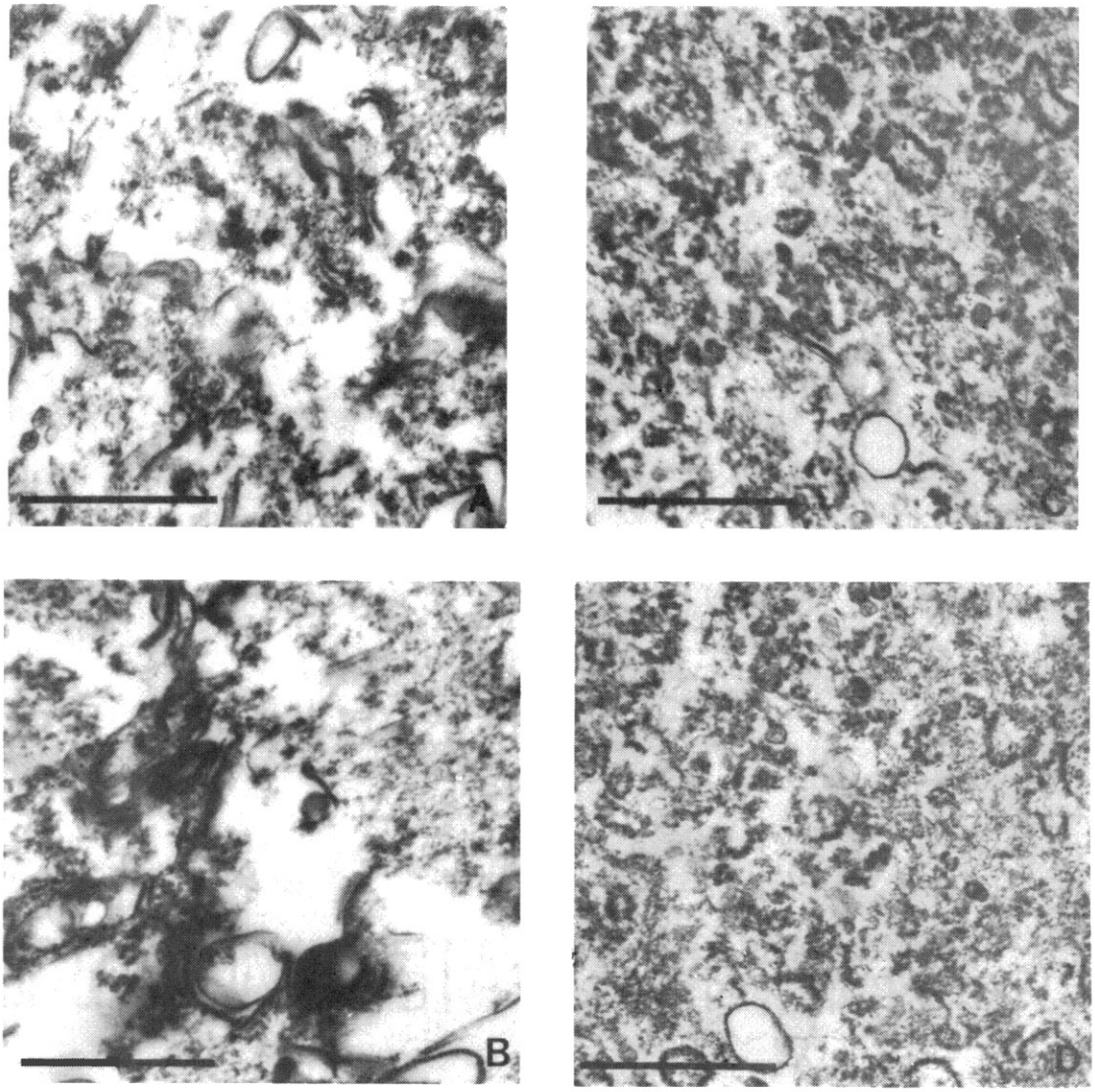
B

Figure 12. SDS PAGE Analysis of MAT-B1 Microvilli, Microvillar Triton Residues and Triton-Soluble Polypeptides.

A) MAT-B1 microvilli, B) MAT-B1 microvillar Triton residue, extracted at a protein concentration of 460 μg ml^{-1}, C) Triton-soluble material from the extraction in B, D) MAT-B1 microvillar Triton residue, extracted at a protein concentration of 115 μg ml^{-1}, E) Triton-soluble material from the extraction in D, F) lane D silver stained, G) lane E silver stained.
Lanes A-E stained with Coomassie blue. The slab gel was 7.5% acrylamide. For further experimental details see the legend of Figure 11. Arrows indicate molecular weight markers for 200,000 daltons, 68,000 daltons and 43,000 daltons.

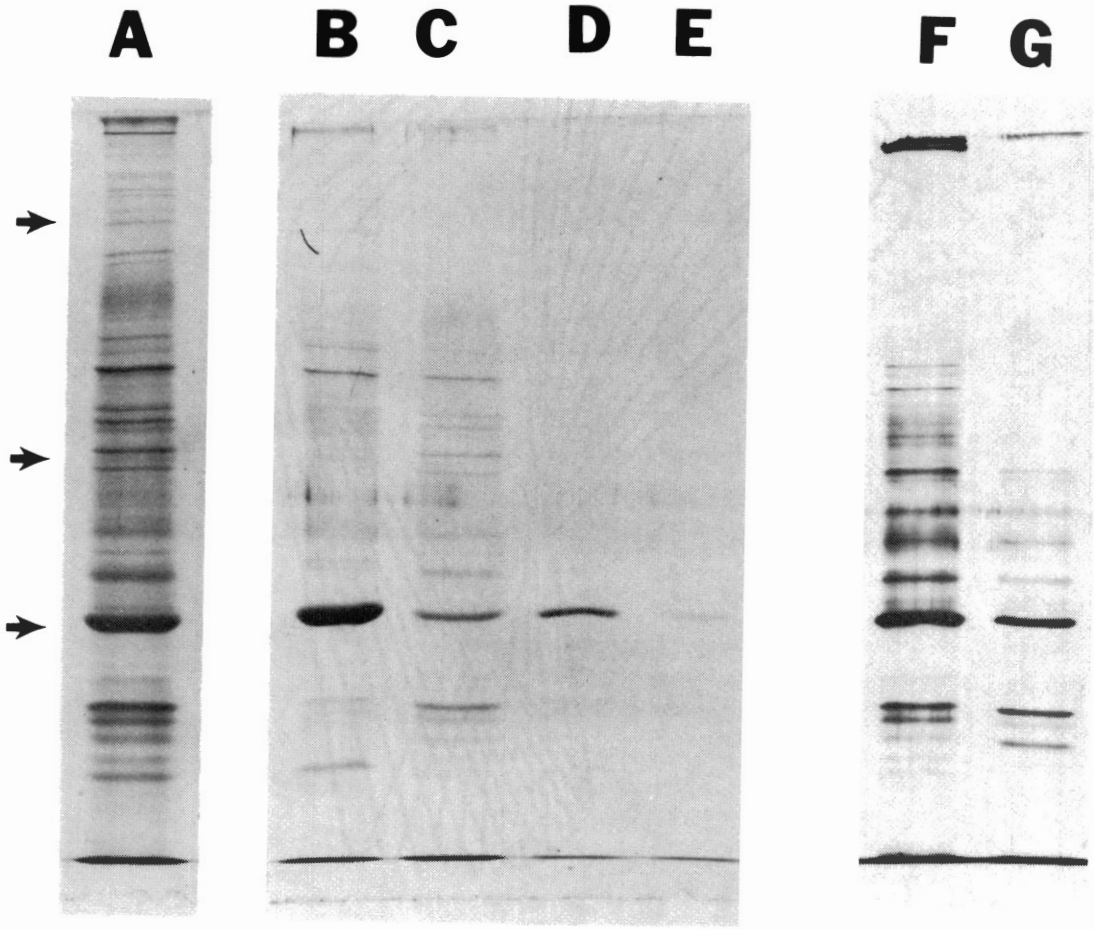
A
B C
D E
F G

Figure 13. Transmission Electron Micrographs of MAT-C1 Microvillar Triton Residues.

MAT-C1 microvilli extracted with 0.2% Triton X-100 at a protein concentration of approximately:
I) 600 μg ml^{-1}. A) Top of the pellet, B) bottom of the pellet.
II) 150 μg ml^{-1}. C) Top of the pellet, D) bottom of the pellet.
Magnifications: A), B), C) and D) 52,500 X. Bars = 0.5 μm. The extraction of metabolically incorporated [^{14}C]-glucosamine was also determined. Amount of label extracted: I) 96.7%, II) 97.7%.

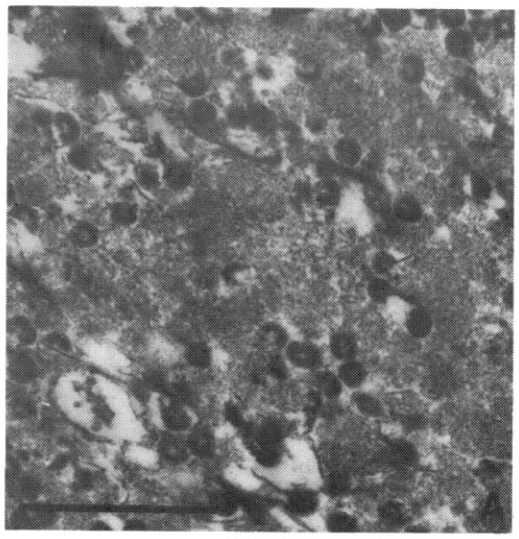
A

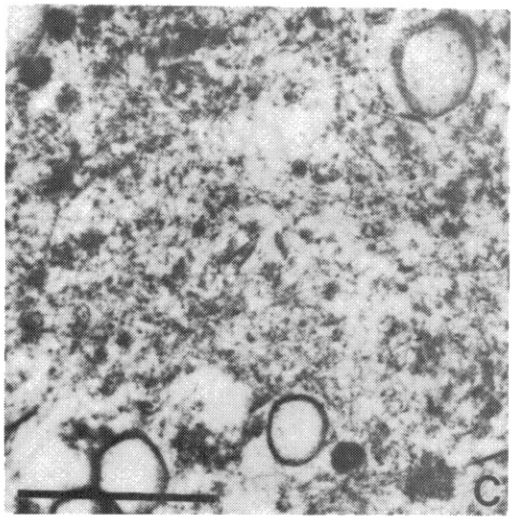
C

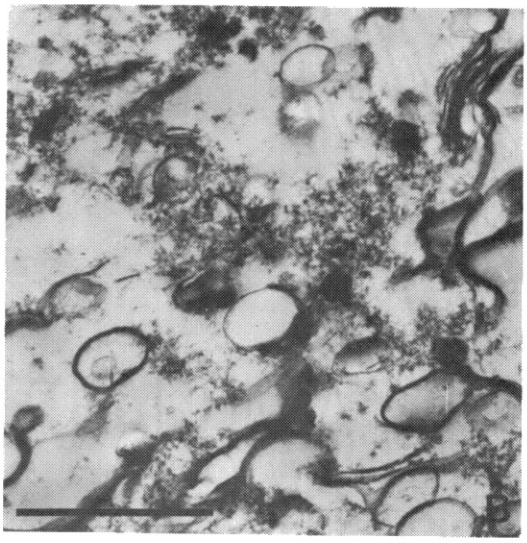
B

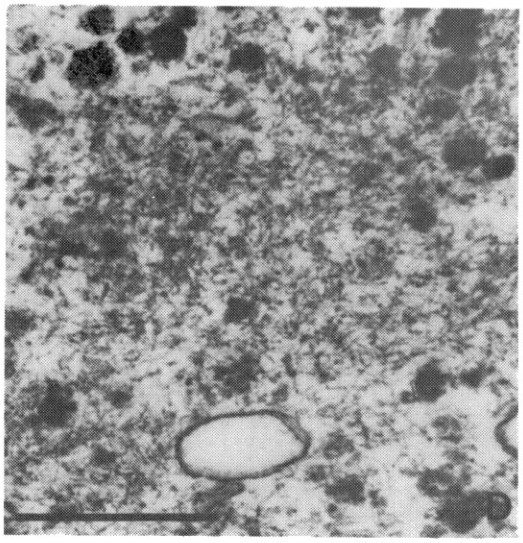
D

clear which, if any, of the structures were entirely within the plane of the section. Any such measurements would be misleading and unreliable. However, using the information gained from the protein composition and the results obtained by negative staining it is probable that this material corresponds to actin microfilaments. Some trilaminar vesicles were present throughout the pellet, although more were found close to the bottom, but there were no multilamellar sheets as there were in the higher protein concentration extractions.

The samples examined by TEM were also analyzed by 1D SDS PAGE (Figures 12 and 14). A large number of polypeptides were present in the MAT-B1 and MAT-C1 microvillar Triton residues produced by extraction at the higher protein concentration. In the lower concentration extraction the major Triton-insoluble polypeptides previously described were found on the 1D gels although CAG was difficult to identify for reasons which have already been discussed.

In view of the TEM observations and the gel analyses it was surprising to note that the extent of the radiolabel extraction was virtually the same at the higher protein concentration as it was at the lower concentration, for both the MAT-B1 and MAT-C1 microvillar fraction (see the legends for Figures 11 and 13). These experiments indicate that the extraction of metabolically incorporated [^{14}C]-glucosamine can not be used to monitor the extent of total membrane solubilization by Triton X-100. Maximal extraction of this radiolabel occurs over a range of protein concentrations and can not be correlated with maximal disappearance of the trilaminar structures observed in TEM.

The putative viruses previously described were present in all the microvillar Triton residues examined by TEM. The membrane, or envelope,

Figure 14. SDS PAGE Analysis of MAT-C1 Microvilli, Microvillar Triton Residues and Triton-Soluble Polypeptides.

A) MAT-C1 microvilli, B) MAT-C1 microvillar Triton residue, extracted at a protein concentration of 600 µg ml^{-1}, C) Triton-soluble material from the extraction in B, D) MAT-C1 microvillar Triton residue, extracted at a protein concentration of 150 µg ml^{-1}, E) Triton-soluble material from the extraction in D, F) lane B silver stained, G) lane C silver stained, H) lane D silver stained, I) lane E silver stained.
Lanes A-E stained with Coomassie blue. The slab gel was 7.5% acrylamide. For further experimental details see the legend of Figure 13. Lower arrow indicates actin, upper arrow indicates 58 K.

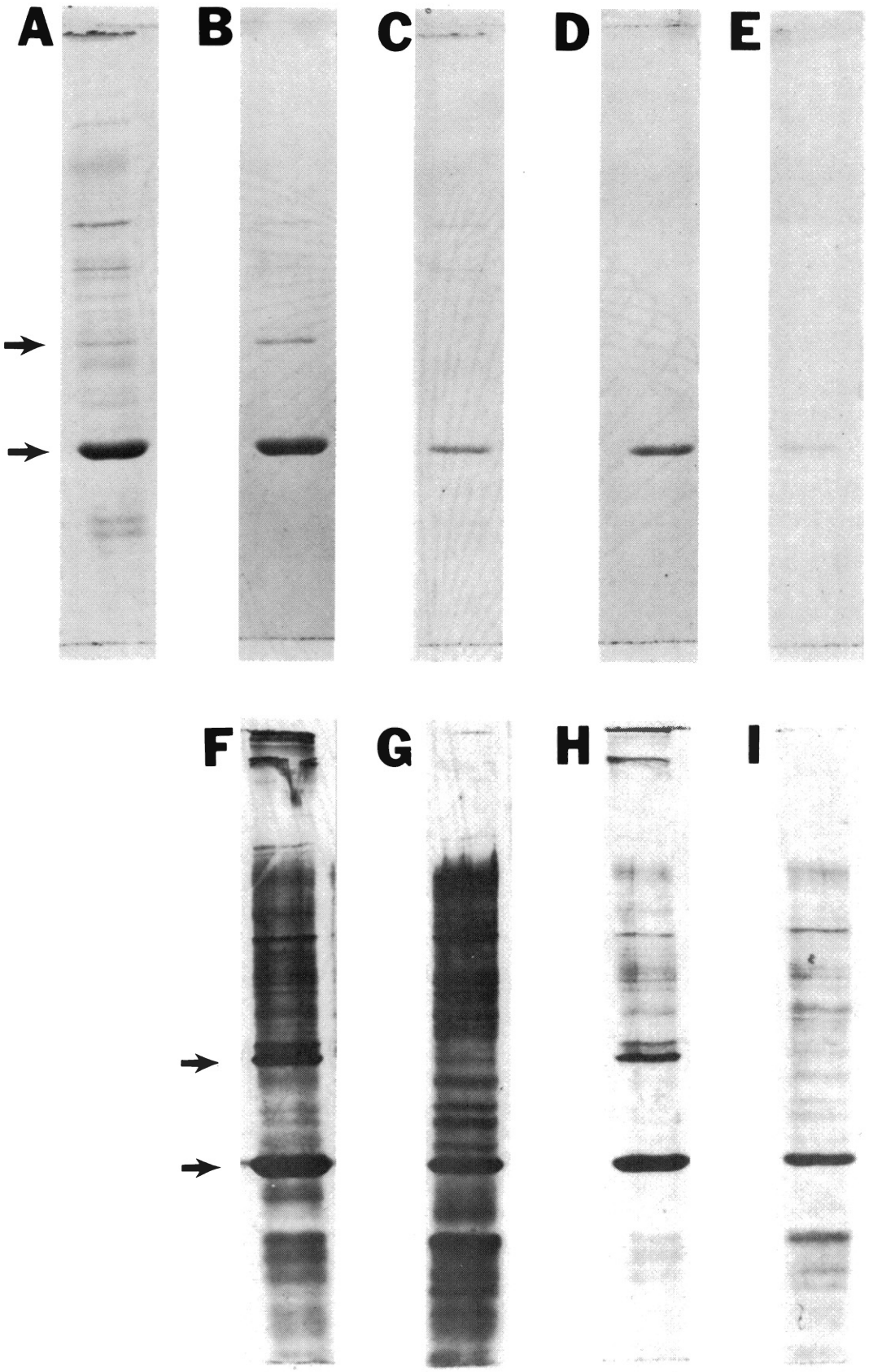
A
B
C
D
E
F
G
H
I

which surrounded each particle appeared to have been removed by the Triton treatment and the only remaining part of each virus was the circular or C-shaped portion. It was not possible to determine from the morphology whether any additional material was present along with these structures. The identity of components which may have contributed to the gel patterns by the particles remains unknown.

Ultrastructure and Protein Composition of MAT-B1 and MAT-C1 Microvillar Membranes

Microvillar membranes were first isolated by Cerra (54). He incubated microvilli in GEM buffer at room temperature for 30 minutes and then homogenized them. A two step differential centrifugation of the homogenate produced a preparation enriched in plasma membrane markers and consisting predominantly of vesicles. Several researchers in this laboratory have employed modified versions of this technique to facilitate their own investigations. It was therefore desirable to determine whether the modified preparations were of comparable morphology and protein composition.

In this study three preparations were examined, including membranes produced by the technique described above. The other two membrane fractions were prepared by incubating microvilli in GEM buffer or GE buffer for 30 minutes at 4°C. Subsequent homogenization and centrifugation of these suspensions produced heterogeneous populations of microvillar fragments in which the microfilaments retained their morphological integrity (Figure 15A and 15B). A membrane vesicle fraction, lacking in microfilaments, was once more obtained when the microvilli were incubated and homogenized in GEM

Figure 15. Transmission Electron Micrographs of MAT-C1 Membrane Fractions.

A) MAT-C1 MF, prepared in GE buffer at 4°C, B) MAT-C1 $MF2_C$, prepared in GEM buffer at 4°C, C) MAT-C1 MF2, prepared in GEM buffer at room temperature. Magnification: A), B) and C) 38,000 X. Bars = 0.5 µm.

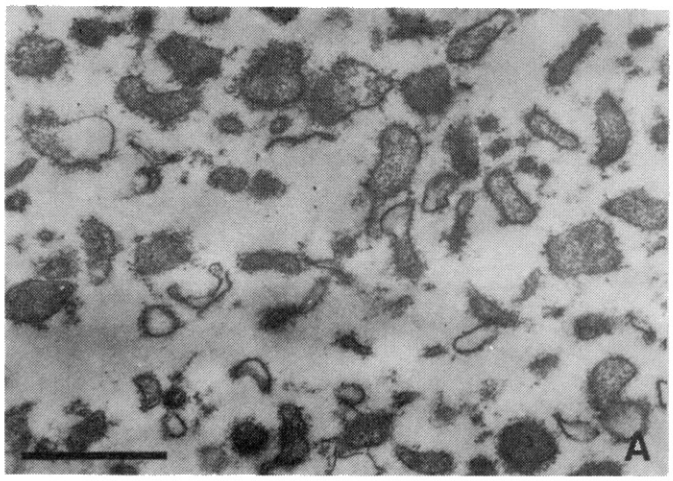
A

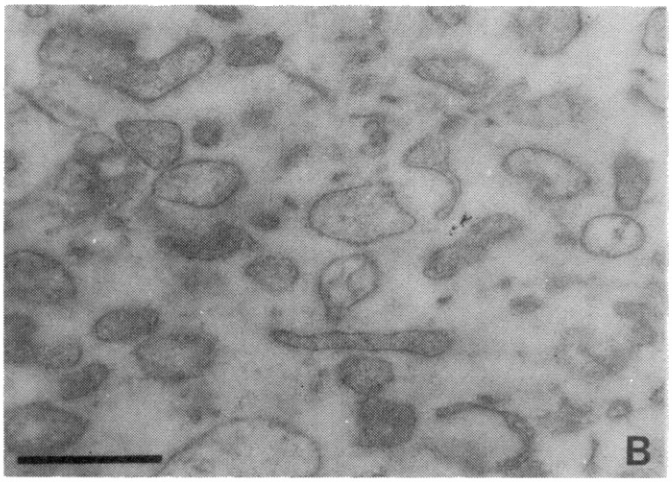
B

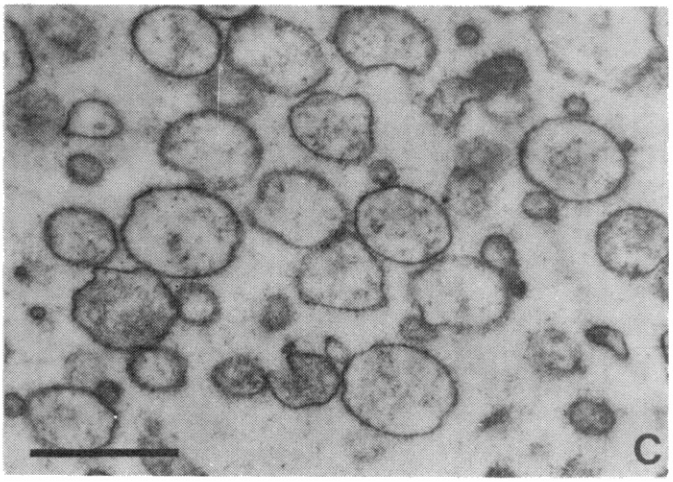
C

buffer at room temperature (Figure 15C).

MAT-C1 microvillar membrane vesicles were approximately 0.25 - 0.4 μm in diameter. Their external surfaces were covered in fibrous material, which was thought to be glycoprotein, while amorphous material was present on the inner surfaces. It is possible that some of the internal components may have been part of the cytoskeleton. However, it is also possible that some of this material may have been derived from the cytoplasm. Cytoplasmic components may have become trapped within the microvilli and subsequently the vesicles.

The membranes around the vesicles in the MAT-C1 preparation appeared to be continuous and this gave the impression that each vesicle was closed (Figure 16C and 16D). However, this was not true for the MAT-B1 microvillar membranes (produced by incubation and homogenization in GEM buffer at room temperature, Figure 16A and 16B). In this case the preparation was a heterogeneous mixture of vesicles and large, open sheets of membrane which had fibrous or amorphous material on both surfaces. Numerous 'double vesicles' (one vesicle inside another) were observed but it was not clear whether one vesicle really was inside the other or whether these images represented a single, invaginated vesicle which crossed the plane of the section in two different regions.

All the microvillar membrane preparations examined in this study were extensively contaminated by viruses. In fact the differential centrifugation technique appeared to enrich the membrane fractions in viral particles.

The 2D gel patterns obtained for MAT-C1 membrane fractions, prepared in GEM or GE buffer at 4°C, were very similar to the pattern

Figure 16. Transmission Electron Micrographs of MAT-B1 and MAT-C1 Microvillar Membrane Preparations.

A) and B) MAT-B1 MF2, prepared in GEM buffer at room temperature, C) and D) MAT-C1 MF2, prepared in GEM buffer at room temperature, E) and F) MAT-C1 MF2 recovered after centrifugation onto a 50% w/v sucrose cushion.
Magnification: A), C), and E) 28,500 X; B), D) and F) 64,000 X. Bars = 0.5 μm.

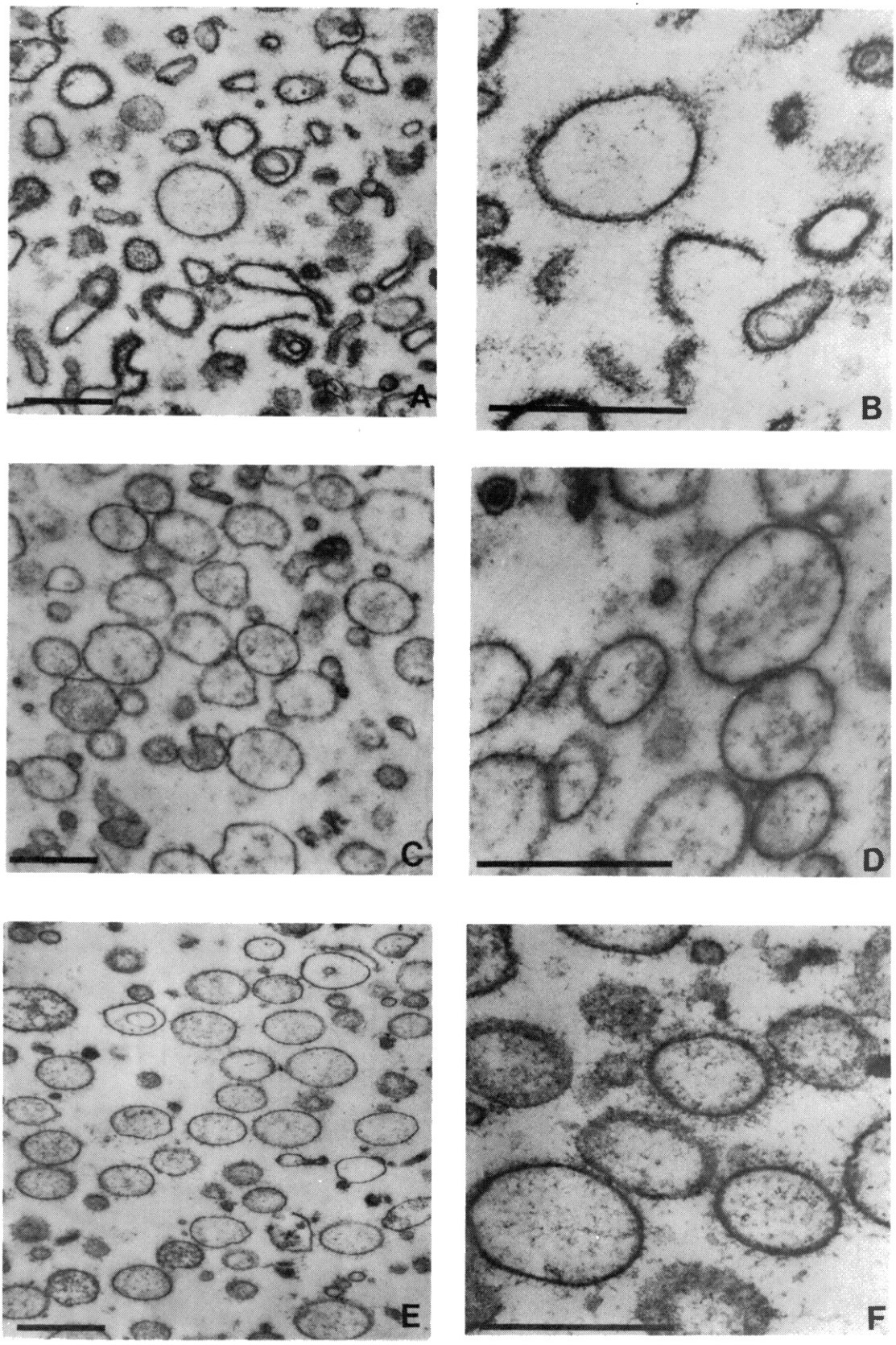
A
B
C
D
E
F

obtained for the microvilli preparation (Figures 17C and 18C). Actin, 58 K, ASGP-2 and CAG were present along with the 100 K daltons component. However, there did appear to be fewer low molecular weight polypeptides than in the whole microvilli preparation. The membrane vesicles also contained the components listed above but in this case there appeared to be an even greater reduction in the number of low molecular weight polypeptides (Figure 18D).

Three other components varied amongst the different preparations. Polypeptides with pI's at approximately pH 6•6, 5•9 and 4•5 and molecular weights in the region of 70 K, 65 K and 50 K daltons were present in the microvilli and microvilli fragments prepared in cold GEM buffer. All three were missing from the microvillar fragments prepared in cold GE buffer and from the membrane vesicles.

MAT-B1 microvillar fragments and membrane vesicles contained actin, CAG, ASGP-2, 100 K and the putative 65 K daltons glycoprotein. 2D gel patterns for the microvillar fragments produced in cold GEM or GE buffer were very similar to each other and to the pattern obtained for the untreated microvilli preparation. The membrane vesicles appeared to show a reduction in the number of low molecular weight components and an increase in a polypeptide with a pI at approximately pH 6•3 which migrated at the upper edge of the β-mercaptoethanol impurity streak.

TEM observations indicated the presence of viruses in these preparations, as already discussed. A number of polypeptides on the 2D gels may have been contributed by these particles. In order to determine the protein composition of the MAT-C1 microvillar membranes alone the vesicle preparation was centrifuged onto a 50% w/v sucrose cushion.

Figure 17. 2D IEF-SDS PAGE Analysis of MAT-B1 and MAT-C1 Membrane Fractions, Prepared in GE Buffer at 4°C, and Triton Residues.

A) MAT-B1 MF, B) MAT-B1 MF Triton residue, C) MAT-C1 MF, D) MAT-C1 MF Triton residue.
All gels silver stained.

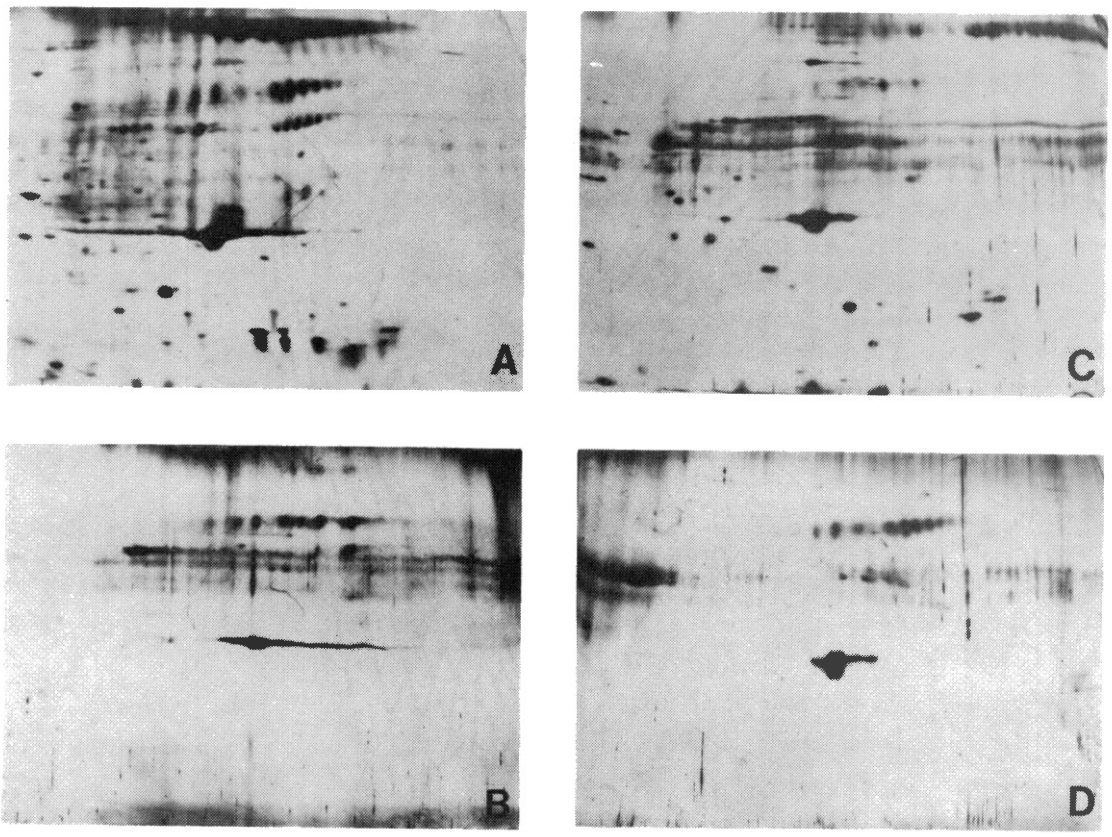
A
C
B
D

Figure 18. 2D IEF-SDS PAGE Analysis of MAT-B1 and MAT-C1 Membrane Fractions, Prepared in GEM Buffer at 4°C or Room Temperature, and MAT-C1 $MF2_c$ Triton Residue.

A) MAT-B1 $MF2_c$, prepared in GEM buffer at 4°C, B) MAT-B1 MF2, prepared in GEM buffer at room temperature, C) MAT-C1 $MF2_c$, prepared in GEM buffer at 4°C, D) MAT-C1 MF2, prepared in GEM buffer at room temperature, E) MAT-C1 $MF2_c$ Triton residue, F) MAT-C1 $MF2_c$ Triton residue. Gels A), C) and E) stained with Coomassie blue, B), D) and F) silver stained.

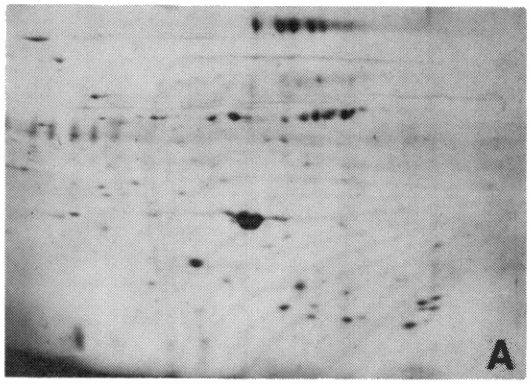
A

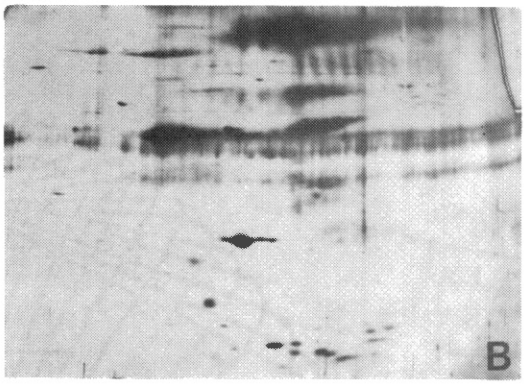
B

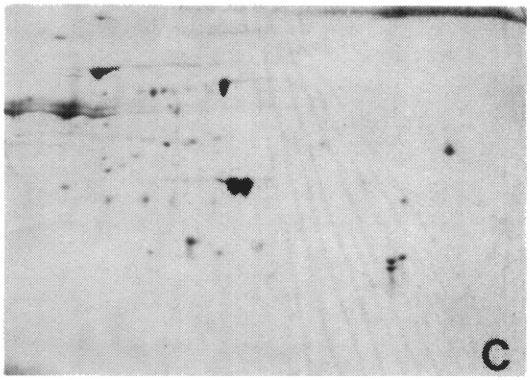
C

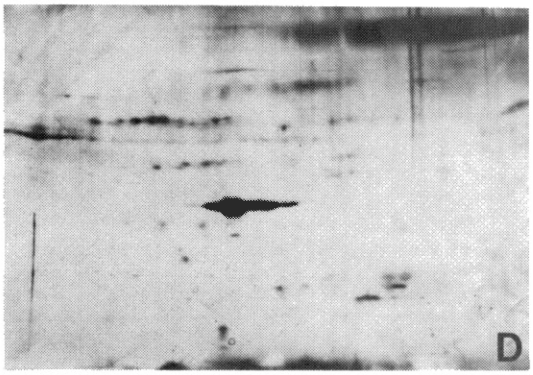
D

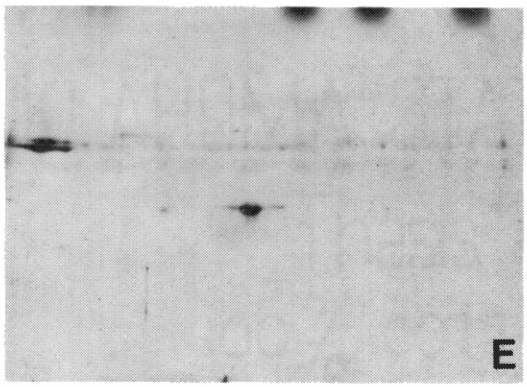
E

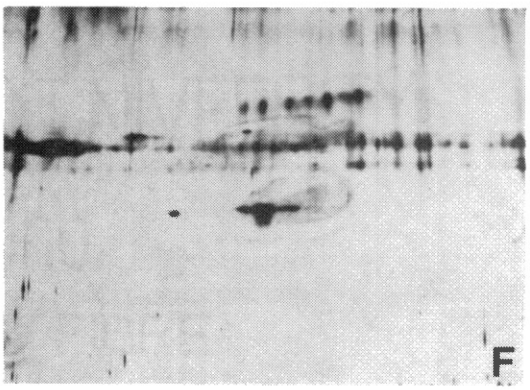
F

It was hoped that the membranes would float at the interface while the viruses would penetrate the cushion. However, TEM observations of the material which collected at the interface revealed that viruses were still present amongst the membrane vesicles (Figure 16E and F). This may have occurred because the density of the sucrose solution was too great, thereby allowing the viruses to float. Alternatively, the gradient may have been overloaded so that the membrane vesicles prevented the viruses from entering the cushion. However, it is also possible that many of the viruses were physically attached to the vesicles, possibly by continuity of their membranes. This proposal is supported in part by the TEM observations of whole cells and microvilli where viral particles could be seen emerging through the plasma membrane. If this is true it implies that this technique could only be used to reduce viral contamination, not to eliminate it. 1D gel analysis of the membrane fraction before and after the attempted purification showed no significant difference (Figure 19), as was expected on the basis of the TEM observations.

Ultrastructure and Protein Composition of MAT-B1 and MAT-C1 Microvillar Membranes Triton Residues

Microvillar membranes or fragments were extracted with Triton X-100 at a protein concentration of approximately 100 $\mu g\ ml^{-1}$. The Triton-insoluble material was then analyzed on 1D or 2D gels.

Triton residues from MAT-B1 microvillar fragments contained primarily actin and CAG (Figure 17B). Additional spots in the region of 60 K daltons molecular weight may have been derived from the

Figure 19. SDS PAGE Analysis of MAT-C1 Microvilli, Microvillar Membranes and Microvillar Membranes after Centrifugation onto a 50% w/v Sucrose Cushion.

A) MAT-C1 microvilli, B) MAT-C1 microvillar membranes, prepared in GEM buffer at room temperature, C) membranes from B after centrifugation onto a 50% w/v sucrose cushion. The gel was 8.0% acrylamide and all the lanes were stained with Coomassie blue. Lower arrow indicates actin, upper arrow indicates 58 K.

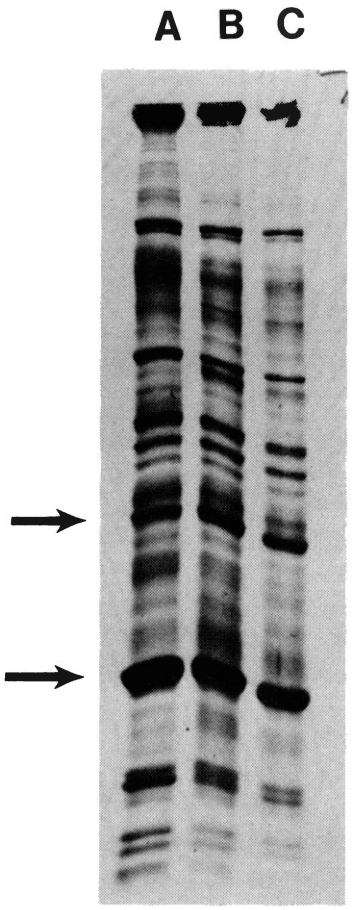
A B C

β-mercaptoethanol impurities. The residue from MAT-B1 membranes (Figure 21) consisted mainly of actin, and several minor components detected only by silver staining. CAG was difficult to identify on 1D gels.

MAT-C1 microvillar fragments and membranes were also extracted under similar conditions. The major Triton-insoluble components in both cases were actin and 58 K. CAG was easily detected by silver staining on the 2D gels (Figures 17D, 18E and 18F) but it was difficult to identify on the 1D gels (Figure 22). Again some minor spots were detected in the 60 K daltons molecular weight region.

The conditions of these extractions were the same as those employed for the microvilli Triton extractions. It was of interest to determine whether the residual material obtained here also contained the trilaminar structures previously observed. Examination of thin sections in the electron microscope indicated that most, if not all the trilaminar structures had been removed from the membrane vesicle Triton residues (Figure 20). There was no material which could be identified as filaments, but this was expected since these were generally absent in the vesicle preparations. High magnification pictures revealed the presence of small regularly sized clusters within the amorphous material. These structures may represent molecular complexes or material which aggregated during the extraction.

The Triton residues obtained from the microvillar membranes of both sublines were heavily contaminated by demembranated viruses. Their possible contribution to the 1D and 2D gel patterns remains unknown.

Figure 20. Transmission Electron Micrographs of MAT-B1 and MAT-C1 Microvillar Membrane Triton Residues.

I) MAT-B1 microvillar membranes extracted with Triton X-100 at a protein concentration of approximately 100 $\mu g\ ml^{-1}$. A) Top of the pellet, B) bottom of the pellet. II) MAT-C1 microvillar membranes extracted with Triton X-100 at a protein concentration of approximately 100 $\mu g\ ml^{-1}$. C) Top of the pellet, D) bottom of the pellet. Magnifications: A), B), C) and D) 52,000 X. Bars = 0.5 µm.

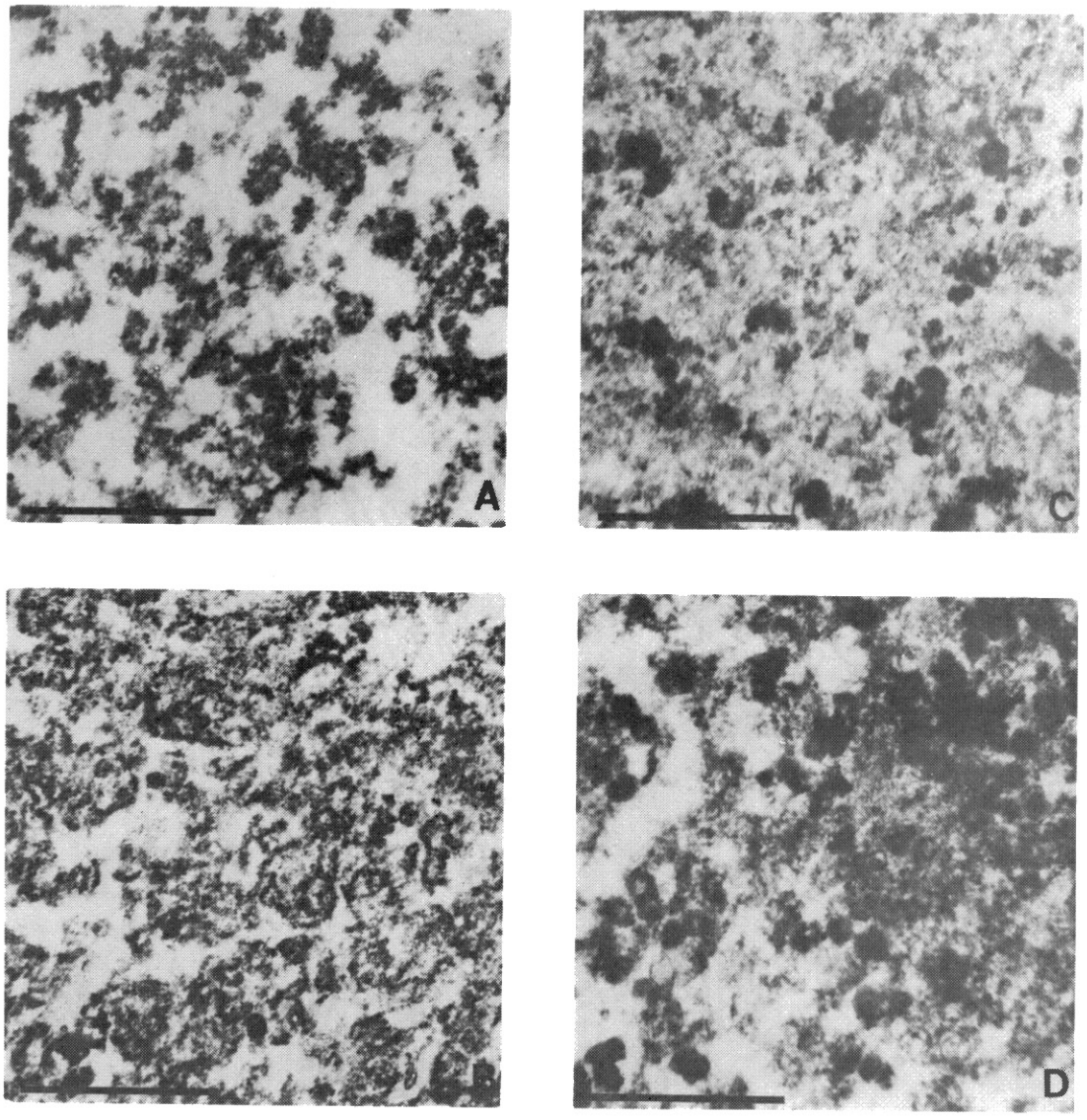
A
C
B
D

Figure 21. SDS PAGE Analysis of MAT-B1 Microvilli, Microvillar Membranes and Microvillar Membrane Triton Residue and Triton-Soluble Polypeptides.

A) MAT-B1 microvilli, B) MAT-B1 MF2, prepared in GEM buffer at room temperature, C) MAT-B1 MF2 from B extracted with 0.2% Triton X-100, D) Triton-soluble material from the extraction in C. The gel was 7.5% acrylamide and all the lanes were silver stained. From top to bottom arrows indicate molecular weight markers for 92,500 daltons, 68,000 daltons and 43,000 daltons.

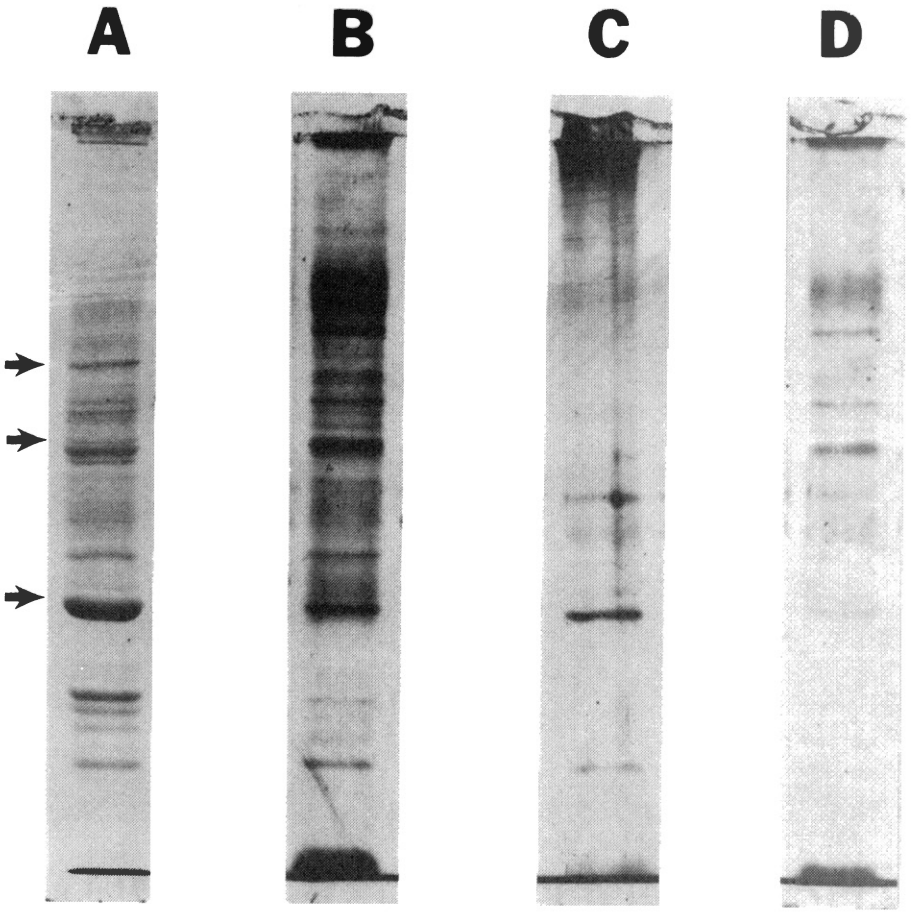
A
B
C
D

Figure 22. SDS PAGE Analysis of MAT-C1 Microvillar Membrane Triton Residue.

A) MAT-C1 MF2 (prepared in GEM buffer at room temperature) Triton residue, extracted with 0.2% Triton X-100, stained with Coomassie blue, B) lane A silver stained. The gel was 10% acrylamide.

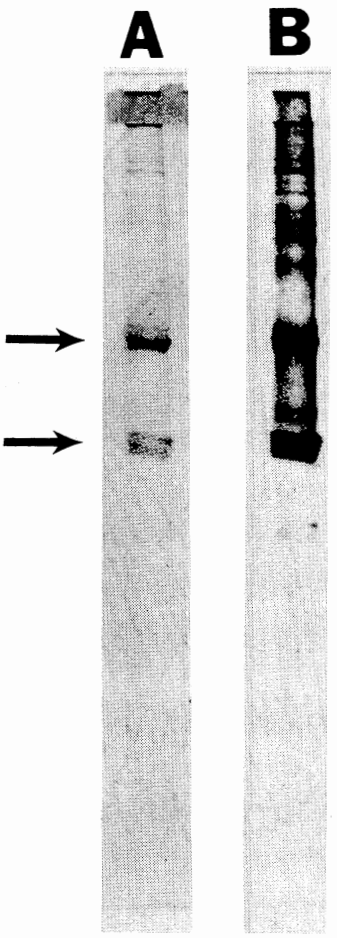
A
B

CHAPTER IV

DISCUSSION

Transmission electron microscopy and light microscopy studies demonstrated that MAT-B1 and MAT-C1 cells contain large reserves of lipid and glycogen. These observations imply that the cells have an abundant supply of nutrients, which might be expected since they are grown in the peritoneal cavity of rats. Both cell types were also found to contain an extensive system of rough endoplasmic reticulum, which suggests that the cells may be synthesizing large quantities of protein. This proposal is consistent with the fact that both MAT-sublines rapidly grow and proliferate in experimental rats.

The mitochondria in the two cell types had strikingly different morphologies. Those in MAT-B1 cells were densely staining, while those in MAT-C1 cells were expanded and more lightly staining. Both types were in the orthodox conformation described by Hackenbrock (63), but this feature was more noticeable in the MAT-C1 organelles because of their greatly expanded appearance. Many tumor cells respire anaerobically so the mitochondria may have been in the conformation in vivo (71). However, it is also possible that the cells were deprived of oxygen during the experimental manipulations prior to fixation. Such conditions could cause mitochondria to change from the condensed to the orthodox conformation. In 1958 Bernhard (72) reported variable mito-

chondrial morphologies in a range of tumor cells. He also noted that aging or degenerating mitochondria often appear to be swollen with a lightly staining matrix. Thus, the expanded morphology of some of the MAT-C1 mitochondria may result because the organelles are necrotic. There is also a possibility that the ultrastructure of the MAT-B1 or the MAT-C1 mitochondria may be a primary lesion of cell transformation.

MAT-B1 cells have many straight microvilli projecting from their cell surface, while MAT-C1 cells have a dense covering of highly branched microvilli (51). MAT-C1 cells are also xenotransplantable whereas MAT-B1 cells are not (50). It has been postulated that the highly branched microvilli may provide a barrier which prevents other cells from approaching too closely (54). This could help to protect the cells from immune responses in the host animal. It has been shown that the presence of highly branched microvilli is more closely correlated with xenotransplantability of 13762 sublines than any other cell surface feature so far examined (73).

Microvilli on the surface of the cells from both sublines contained variable numbers of 70 Å filaments, which were thought to be actin filaments. Microfilaments in the microvilli of intestinal brush border cells, or on the surface of fertilized purple sea urchin eggs, are fastened into a bundle and extend the entire length of each microvillus (26, 74). However, the 70 Å filaments examined in this study were often considerably shorter than the microvilli and they were not organized into bundles. The ends of many of the filaments appeared to be associated with the membrane but there was no dense tip material to anchor all the filaments to the distal end of the microvillus; neither was there a terminal web to anchor the filaments into the cell

body. The unusual morphological features of the MAT-B1 and MAT-C1 microvilli warrant further investigation, as they represent an alternative structural arrangement which may be more representative of the microvilli which occur transiently on a variety of cells grown in culture (75).

2D IEF-SDS PAGE analysis of MAT-B1 and MAT-C1 microvillar proteins revealed the presence of two spots, with slightly different pI's, at a molecular weight of approximately 43,000 daltons. These are believed to be the β and γ isomers of actin which have been found in many nonmuscle cells (24). The two forms are usually present together but in variable ratios. It has been suggested that isoactins may have different functional roles since α-actin is the predominant form in skeletal muscle, while γ-actin is the major isomer in smooth muscle. However, there is little evidence to support or refute similar functional divisions within nonmuscle cells (76, 77).

Actin was the major Triton-insoluble material derived from the microvilli of both sublines, and 70 Å filaments were observed in the Triton residues examined by negative staining in the electron microscope. Numerous branched microfilaments were observed in the negatively stained material and in the intact and isolated microvilli. Since actin filaments are more usually straight it seems plausible that the branching points may be associated with, and possibly stabilized by, an actin binding protein. A polypeptide with an apparent molecular weight of approximately 100 K daltons was present in the microvilli and the microvillar Triton residues. This component may be α-actinin, which is known to be present in the MAT-C1 microvilli (65). Although clearly speculative, it is possible that this polypeptide may be

associated with the filament branching points. In 1976 Lazarides (78) used indirect immunofluorescence to determine the distribution of actin, tropomyosin and α-actinin in spreading rat embryo cells grown in culture. He found that an intricate dome-shaped lattice-work of tropomyosin containing actin filaments was present in the cytoplasm surrounding the nucleus. The lattice was attached to the plasma membrane by different actin filaments which contained both tropomyosin and α-actinin. However, he observed that the vertices of the lattice-work (the points where the microfilaments appeared to converge, or branch) contained only actin and α-actinin, suggesting that this polypeptide may play a role in stabilizing the microfilament interactions in these regions.

The major cell surface glycoproteins, ASGP-1 and ASGP-2, were almost completely extracted from the microvilli by the Triton X-100 treatment (69). Previous studies have shown that greater than 70% of metabolically incorporated [^{14}C]-glucosamine becomes associated with ASGP-1 in the MAT-B1 and MAT-C1 cells (69). As already discussed, the maximum extraction of the incorporated radiolabel can not be correlated with the loss of trilaminar structures seen in TEM. ASGP-1 and ASGP-2 have been isolated as a complex and ASGP-2 is believed to be an integral membrane protein (E. Cerven, unpublished observations). The results obtained here suggest that the nonionic detergent may be able to remove certain integral membrane molecules without completely disrupting the membrane structure.

Unlike ASGP-1 and ASGP-2, CAG was present in the Triton residues of MAT-B1 and MAT-C1 microvilli. This data, in combination with many other studies performed in this laboratory (discussed in Chapter III),

suggests that CAG may be a transmembrane glycoprotein associated with the cytoskeleton. There is also preliminary data which suggests that CAG may be involved in lectin receptor redistribution (R. M. Helm, unpublished observations). The information gathered so far appears to imply that CAG may fulfill the role of the X protein(s) described by Bourguignon and Singer (18).

MAT-C1 microvilli contain a 58 K polypeptide which is reduced or absent from MAT-B1 microvilli. Previous studies indicated that this protein may be associated with the cytoskeleton and the membrane (52). It has been postulated that 58 K may have a restrictive influence on surface receptor mobility in the MAT-C1 cells, possibly by stabilizing the cytoskeleton.

Microvillar membrane fractions were prepared in hypotonic buffer at 4°C and room temperature. Only the fractions prepared at room temperature contained predominantly vesicles lacking in microfilaments. The 4°C preparations contained microvillar fragments which retained their microfilaments. When the fragments were extracted with Triton X-100 the residues contained the same components that were found in the microvillar Triton residues. MAT-B1 and MAT-C1 membrane vesicle Triton residues contained actin, and in the latter case 58 K was also present. Although CAG was difficult to identify on 1D gels it appears that this polypeptide was not a major component of membrane vesicle Triton residues. If CAG is anchored to the cytoskeleton via a direct or indirect interaction with actin filaments, then removing the actin filaments may release CAG from its anchorage sites, thus allowing it to be more easily extracted by Triton X-100, in a similar way to other integral membrane proteins (70).

The MAT-B1 and MAT-C1 cells, and all the preparations derived from them, were contaminated by particles which were identified as viruses on the basis of their morphology. Those in the MAT-B1 preparations may, or may not, have been the same as those in the MAT-C1 preparations. The solid 13762 rat mammary adenocarcinoma was induced by a chemical carcinogen. If the original tumor was free of viruses it is possible that the sublines became infected during in vivo passage.

The extracellular viral particles observed in this study appeared to be similar to the RNA containing mouse mammary tumor virus (MMTV), which is a type B particle according to the classification of Bernhard (64). In 1970 Drohan and Schlom (79) conducted MMTV RNA-rodent DNA hybridization experiments which showed that the genomes of feral rats and several laboratory strains of rats contained MMTV related sequences. These sequences are endogenous and transmitted through the germ line. However, they also showed that the DNA of certain colonies of Fischer (344) rats, which are the same type used to passage the MAT-B1 and MAT-C1 cells, contained additional MMTV-related sequences. These were shown to be related to the infectiously transmitted, tumor associated sequences of MMTV (C3H), a highly oncogenic virus (79-81). Thus, the MMTV related sequences in Fischer (344) rats can be of two types. One set can be transmitted through the germ line, while the other set appears to be capable of horizontal transmission in an infectious manner. It is possible that one or more rats used for the in vivo passages may have carried an infectious viral form which subsequently contaminated the entire subline(s).

The particles observed in this study appeared to be type B viruses

but it is possible that the cells may have been contaminated by both type B and type C particles. Such an occurrence is not unprecedented since mouse mammary tumors grown in culture frequently produce MMTV and concomitantly release type C, murine leukemia viruses (82). Although type B and type C particles have different morphologies it is doubtful that they could be adequately distinguished at the level of resolution attainable here. A detailed ultrastructural study, specifically directed towards the viruses, would be necessary in order to classify them accurately.

RNA tumor viruses mature at pre-existing plasma membranes and acquire a membrane envelope as they bud into the extracellular environment. The envelopes of RNA tumor viruses are typically covered by spikes, or projections, which have been identified as glycoproteins in a number of cases (83). In order for these molecules to be transferred to the viral membrane they must first be expressed and assembled in the plasma membrane of the host cell. It is possible that some of the polypeptides detected in the MAT-B1 and MAT-C1 microvilli and membrane preparations may be virally encoded. In view of this it would be of interest to isolate the particles and characterize their molecular composition.

CHAPTER V

SUMMARY AND CONCLUSIONS

Cells from the MAT-C1 subline of the 13762 rat mammary adenocarcinoma have a dense covering of highly branched microvilli, relatively immobile cell surface receptors and are xenotransplantable. The MAT-B1 subline consists of cells with unbranched microvilli and highly mobile surface receptors. This subline is not xenotransplantable. Previous studies have shown that the presence of highly branched microvilli is the only cell surface feature, examined so far, which can be positively correlated with xenotransplantability (73). Since cell surface morphology appears to be a major factor in determining the survivability of the cells in experimental animals, it is important to understand how the highly branched microvilli are constructed, and what factor(s) cause them to be different from the microvilli of MAT-B1 cells.

The microvilli from both sublines are apparently constructed differently from those of the highly differentiated intestinal brush border cells and fertilized sea urchin eggs. 70 Å filaments in the microvilli of the MAT-sublines examined here were variable in number and did not appear to be fastened into a tight bundle. No structures were detected which were equivalent to the dense tip material, or terminal web, of brush border microvilli, but some of the microfilaments did appear to be associated with the membrane and many were

branched. A comparison of the microvilli preparations on 2D IEF-SDS PAGE confirmed that a 58 K polypeptide was present in the MAT-C1 microvilli, which was reduced or absent in the MAT-B1 microvilli preparations. This technique revealed the presence of a 78 K component in the microvilli of both sublines. The evidence gathered so far appears to imply that 78 K is a cytoskeletal associated glycoprotein. CAG and actin were present in the Triton residues from MAT-B1 and MAT-C1 microvilli, and in the latter case 58 K was also present.

Microvillar membranes were prepared in GEM buffer at room temperature. Microfilaments were largely absent from these preparations, although actin was still present when they were analyzed by gel electrophoresis. CAG was present in the preparations from both sublines, along with 58 K in the case of MAT-C1 membranes. When these preparations were extracted with Triton X-100, the MAT-B1 residue contained predominantly actin, while the MAT-C1 preparation contained actin and 58 K. CAG did not appear to be a major component in either of the Triton residues. This data may imply that CAG can be partially extracted from the membranes when the microfilaments have been removed. Alternatively, the apparently reduced amount of CAG may have been an effect of the low protein concentrations applied to the gels.

Both sublines were found to be contaminated by putative viral particles. Such particles were also found in the microvilli, membrane fractions and Triton residue preparations. The data presented in this study suggests that the particles may be type B viruses, but further investigations would be necessary in order to classify them accurately. It would be of interest to isolate and characterize the particles. Thus,

it could be determined whether those in the MAT-B1 cells are the same as those in the MAT-C1 cells. This would also enable the viral associated components to be distinguished from those which are indigenous to the cells of each subline. The contribution of the viruses to the phenomenon of xenotransplantability also remains to be determined.

A SELECTED BIBLIOGRAPHY

(1) Abercrombie, M., Heaysman, J. E. M., and Pegrum, S. M. (1971) Exp. Cell Res., 67, 359-367.

(2) Edelman, G. M. (1976) Sci., 192, 218-226.

(3) Hughes, R. C. (1975) Essays in Biochem., 11, 1-36.

(4) Nicolson, G. L., and Poste, G. (1976) New Engl. J. Med., 295, 253-258.

(5) Frye, L. D., and Edidin, M. (1970) J. Cell Sci., 7, 319-335.

(6) Singer, S. J., and Nicolson, G. L. (1972) Sci., 175, 720-731.

(7) Taylor, R. B., Duffus, W. P. H., Raff, M. C. and de Petris, S. (1971) Nature New Biol., 233, 225-229.

(8) Schreiner, G. F., and Unanue, E. R. (1976) Adv. Immunol., 24, 37-165.

(9) Nicolson, G. L. (1976) Biochim. Biophys. Acta, 457, 57-108.

(10) Ukena, T. E., and Berlin, R. D. (1972) J. Exp. Med., 136, 1-7.

(11) Yahara, I., and Edelman, G. M. (1975) Exp. Cell Res., 91, 125-142.

(12) Nicolson, G. L., and Poste, G. (1976) New Engl. J. Med., 295, 197-203.

(13) Berlin, R. D., and Oliver, J. M. (1978) J. Cell Biol., 77, 789-804.

(14) Berlin, R. D., Oliver, J. M., Ukena, T. S., and Yin, H. H. (1974) Nature, 247, 45-46.

(15) Ji, T. H. (1974) J. Biol. Chem., 249, 7841-7847.

(16) Ji, T. H., and Nicolson, G. L. (1974) Proc. Natl. Acad. Sci. U.S.A., 71, 2212-2216.

(17) Nicolson, G. L., and Painter, R. G. (1973) J. Cell Biol., 59, 395-406.

(18) Bourguignon, L. Y. W., and Singer, S. J. (1977) Proc. Natl. Acad. Sci. U.S.A., 74, 5031-5035.

(19) Sabatini, D. D., Bensch, K., and Barrnett, R. J. (1963) J. Cell Biol., 17, 19-58.

(20) Snyder, J. A., and McIntosh, J. R. (1976) Ann. Rev. Biochem., 45, 669-720.

(21) Lazarides, E. (1980) Nature, 283, 249-255.

(22) Lazarides, E. (1975) J. Histochem. Cytochem., 23, 507-528.

(23) Tilney, L. G., and Mooseker, M. (1971) Proc. Natl. Acad. Sci. U.S.A., 68, 2611-2615.

(24) Garrels, J. I., and Gibson, W. (1976) Cell, 9, 793-805.

(25) Ishikawa, H., Bischoff, R., and Holdzer, H. (1969) J. Cell Biol., 43, 312-328.

(26) Mooseker, M. S. and Tilney, L. G. (1975) J. Cell Biol., 67, 725-743.

(27) Schollmeyer, J. V., Goll, D. E., Tilney, L. G., Mooseker, M., Robson, R., and Stromer, M. (1974) J. Cell Biol., 63, 304a.

(28) Bretscher, A., and Weber, K. (1978) Exp. Cell Res., 116, 397-407.

(29) Geiger, B., Tokuyasu, K. T., and Singer, S. J. (1979) Proc. Natl. Acad. Sci. U.S.A., 76, 2833-2837.

(30) Matsudaira, P. T., and Burgess, D. R. (1979) J. Cell Biol., 83, 667-673.

(31) Bretscher, A., and Weber, K. (1980) Cell, 20, 839-847.

(32) Glenney, J. R., Kaulfus, P., and Weber, K. (1981) Cell, 24, 471-480.

(33) Bretscher, A., and Weber, K. (1980) J. Cell Biol., 86, 335-340.

(34) Mescher, M. F., Jose, M. J. L., and Balk, S. P. (1981) Nature, 289, 139-144.

(35) Dodge, J. T., Mitchell, C., and Hanahan, D. J. (1963) Arch. Biochem. Biophys., 100, 119-130.

(36) Anderson, A. J. (1979) J. Biol. Chem., 254, 939-944.

(37) Fairbanks, G., Steck, T. L., and Wallach, D. F. H. (1971) Biochem., 10, 2606-2617.

(38) Shotton, D., Burke, B., and Branton, D. (1978) Biochim. Biophys. Acta, 536, 313-317.

(39) Goodman, S., and Weidner, S. (1980) J. Biol. Chem., 255, 8082-8086.

(40) Ungewickell, E., Bennett, P. M., Calvert, R., Ohanian, V., and Gratzer, W. B. (1979) Nature, 280, 811-814.

(41) Cohen, C. M., Tyler, J. M. and Branton, D. (1980) Cell, 21, 875-883.

(42) Liu, S. C., Sepe, S., Crusberg, T., and Packe, J. (1978) Fed. Proc., 37, 1508.

(43) Bennett, V., and Branton, D. (1977) J. Biol. Chem., 252, 2753-2763.

(44) Bennett, V. (1978) J. Biol. Chem., 253, 2292-2299.

(45) Bennett, V., and Stenbuck, P. J. (1979) J. Biol. Chem., 254, 2533-2541.

(46) Luna, E. J., Kidd, G. H., and Branton, D. (1979) J. Biol. Chem., 254, 2526-2632.

(47) Yu, J., and Goodman, S. R. (1979) Proc. Natl. Acad. Sci. U.S.A., 76, 2340-2344.

(48) Bennett, V., and Stenbuck, P. J. (1979) Nature, 280, 468-473.

(49) Huggins, J. W., Trenbeath, T. P., Yeltman, D. R. and Carraway, K. L. (1980) Exp. Cell Res., 127, 31-46.

(50) Sherblom, A. P., Huggins, J. W., Chestnut, R. W., Buck, R. L., Ownby, C. L., Dermer, G. B., and Carraway, K. L. (1980) Exp. Cell Res., 126, 417-426.

(51) Carraway, K. L., Doss, R. C., Huggins, J. W., and Carraway, C. A. C. (1979) J. Cell Biol., 83, 529-543.

(52) Carraway, C. A. C., Cerra, R. F., and Carraway, K. L. (1981) J. Cell Biol., 91, 253A.

(53) Cerra, R. F., Carraway, C. A. C., and Carraway, K. L. (1981) J. Cell Biol., 91, 293A.

(54) Cerra, R. F. "Control of Cell Surface Organization in Ascites Tumor Cells." (Unpub. Ph.D. dissertation, Oklahoma State University, 1981.)

(55) Lowry, O. H., Rosebrough, J. N., Farr, A. L., and Randall, R. J. (1951) J. Biol. Chem., 193, 265-275.

(56) O'Farrell, P. H. (1975) J. Biol. Chem., 250, 4007-4021.

(57) Wilson, D. L., Hall, G. E., Stone, G. C., and Rubin, R. W. (1977) Anal. Bioch., 83, 33-44.

(58) Leonardi, C. L., Warren, R. H., and Rubin, R. W. (1982) Biochim. Biophys. Acta, 720, 154-162.

(59) Rubin, R. W., and Leonardi, C. L. Methods in Enzymology (in press).

(60) Goldman, D., Sedman, A. S., and Ebert, M. H. (1981) Sci., 211, 1437-1438.

(61) Hayat, M. A. Principles and Techniques of Electron Microscopy. Biological Applications. Vol. I, 1st Ed. Van Nostrand Reinhold Co., 1970, pp. 342-434.

(62) Lillie, R. D., and Fullmer, H. M. Histologic Technic and Practical Histochemistry. 4th Ed. McGraw-Hill Book Co., Inc., 1976, pp. 617.

(63) Hackenbrock, C. R. (1968) J. Cell Biol., 37, 345-369.

(64) Bernhard, W. (1960) Cancer Res., 20, 712-727.

(65) Carraway, K. L., Huggins, J. W., Cerra, R. F., Yeltman, D. R., and Carraway, C. A. C. (1980) Nature, 285, 508-510.

(66) Mukherjee, T. M., and Staehelin, L. A. (1971) J. Cell Sci., 8, 573-599.

(67) Korn, E. D. (1978) Proc. Natl. Acad. Sci., U.S.A., 75, 588-599.

(68) Wilson, D. L. Handbook of Neurochemistry. Vol. II, 2nd Ed. Plenum, Ed. A. Lajtha (in press).

(69) Sherblom, A. P., and Carraway, K. L. (1980) J. Biol. Chem., 255, 12051-12059.

(70) Sheetz, M. (1979) Biochim. Biophys. Acta, 557, 122-134.

(71) Makan, N. R., and Heppel, L. A. (1978) J. Cell Physiol., 96, 87-94.

(72) Bernhard, W. (1958) Cancer Res., 18, 491-509.

(73) Howard, S. C., Hull, S. R., Huggins, J. W., Carraway, C. A. C., Carraway, K. L. J. Natl. Cancer Inst. (in press).

(74) Burgess, D. R., and Schroeder, T. E. (1977) J. Cell Biol., 74, 1032-1037.

(75) Yamada, K. M., Ohanian, S. H., Pastan, I. (1976) Cell, 9, 241-245.

(76) Rubenstein, P. A. (1981) Arch. Biochem. Biophys., 210, 598-608.

(77) Rubenstein, P., Ruppert, T., and Sandra, A. (1982) J. Cell Biol., 92, 164-169.

(78) Lazarides, E. (1976) J. Cell Biol., 68, 202-219.

(79) Drohan, W., and Schlom, J. (1979) J. Natl. Cancer Inst., 62, 1279-1286.

(80) Drohan, W., and Schlom, J. (1979) J. Virol., 31, 53-62.

(81) Drohan, W., Keltman, R., Colcher, D., and Schlom, J. (1977) J. Virol., 21, 986-995.

(82) Schlom, J. Molecular Biology of RNA Tumor Viruses. Ed. Stephenson. Academic Press, 1980, pp. 449.

(83) Lenard, J., and Compans, R. W. (1974) Biochim. Biophys. Acta, 344, 51-94.

VITA

Julie Roberts Craik

Candidate for the Degree of

Master of Science

Thesis: MORPHOLOGY AND PROTEIN COMPOSITION OF TWO SUBLINES OF THE 13762 RAT MAMMARY ADENOCARCINOMA

Major Field: Biochemistry

Biographical:

Personal Data: Born in Wakefield, Yorkshire, England, February 23, 1955, the daughter of Mr. and Mrs. L. Roberts.

Education: Graduated from Normanton Grammar School, Normanton, Yorkshire, England in July, 1973; received the Bachelor of Arts degree in Biology from the University of York, York, England in July, 1976; received the Post-Graduate Certificate in Education from the University of York, York, England in July, 1977; completed the requirements for the Master of Science degree at Oklahoma State University in July, 1982.

Professional Experience: Teacher of Biology and General Science at Wales Comprehensive School, Yorkshire, England, from September, 1977 to July, 1980; Graduate Research Assistant, Department of Biochemistry, Oklahoma State University, Stillwater, Oklahoma, from September, 1980 to May, 1981; Graduate Research Assistant, Department of Anatomy, School of Medicine, University of Miami, Florida, from September, 1981 to May, 1982.